



# The importance of topography-controlled sub-grid process heterogeneity and semi-quantitative prior constraints in distributed hydrological models

Remko C. Nijzink<sup>1</sup>, Luis Samaniego<sup>2</sup>, Juliane Mai<sup>2</sup>, Rohini Kumar<sup>2</sup>, Stephan Thober<sup>2</sup>, Matthias Zink<sup>2</sup>, David Schäfer<sup>2</sup>, Hubert H. G. Savenije<sup>1</sup>, and Markus Hrachowitz<sup>1</sup>

<sup>1</sup>Delft University of Technology, Stevinweg 1, 2628 CN Delft, the Netherlands

<sup>2</sup>UFZ – Helmholtz Centre for Environmental Research, Permoserstraße 15, 04318 Leipzig, Germany

Correspondence to: R. C. Nijzink (r.c.nijzink@tudelft.nl)

Received: 11 November 2015 – Published in Hydrol. Earth Syst. Sci. Discuss.: 21 December 2015

Revised: 3 March 2016 – Accepted: 4 March 2016 – Published: 17 March 2016

**Abstract.** Heterogeneity of landscape features like terrain, soil, and vegetation properties affects the partitioning of water and energy. However, it remains unclear to what extent an explicit representation of this heterogeneity at the sub-grid scale of distributed hydrological models can improve the hydrological consistency and the robustness of such models. In this study, hydrological process complexity arising from sub-grid topography heterogeneity was incorporated into the distributed mesoscale Hydrologic Model (mHM). Seven study catchments across Europe were used to test whether (1) the incorporation of additional sub-grid variability on the basis of landscape-derived response units improves model internal dynamics, (2) the application of semi-quantitative, expert-knowledge-based model constraints reduces model uncertainty, and whether (3) the combined use of sub-grid response units and model constraints improves the spatial transferability of the model.

Unconstrained and constrained versions of both the original mHM and mHMtopo, which allows for topography-based sub-grid heterogeneity, were calibrated for each catchment individually following a multi-objective calibration strategy. In addition, four of the study catchments were simultaneously calibrated and their feasible parameter sets were transferred to the remaining three receiver catchments. In a post-calibration evaluation procedure the probabilities of model and transferability improvement, when accounting for sub-grid variability and/or applying expert-knowledge-based model constraints, were assessed on the basis of a set of hydrological signatures. In terms of the Euclidian distance to

the optimal model, used as an overall measure of model performance with respect to the individual signatures, the model improvement achieved by introducing sub-grid heterogeneity to mHM in mHMtopo was on average 13 %. The addition of semi-quantitative constraints to mHM and mHMtopo resulted in improvements of 13 and 19 %, respectively, compared to the base case of the unconstrained mHM. Most significant improvements in signature representations were, in particular, achieved for low flow statistics. The application of prior semi-quantitative constraints further improved the partitioning between runoff and evaporative fluxes. In addition, it was shown that suitable semi-quantitative prior constraints in combination with the transfer-function-based regularization approach of mHM can be beneficial for spatial model transferability as the Euclidian distances for the signatures improved on average by 2 %. The effect of semi-quantitative prior constraints combined with topography-guided sub-grid heterogeneity on transferability showed a more variable picture of improvements and deteriorations, but most improvements were observed for low flow statistics.

## 1 Introduction

A better understanding of the link between landscape heterogeneity and its impact on process dynamics of catchments is urgently required to develop more robust catchment-scale rainfall–runoff models that have the skill to adequately reproduce the observed system response dynamics, even

for catchments where no calibration data are available. Besides heterogeneity in the system boundary conditions, including amongst others topography, vegetation or geology (e.g. Knudsen, 1986; Rodríguez-Iturbe, 2006; Tromp-van Meerveld, 2006), climatic variables, i.e. the forcing of models such as precipitation and evaporation, typically exhibit considerable spatial variability (e.g. Obled, 1994; Singh, 1997; Winsemius et al., 2008; Hrachowitz and Weiler, 2011). Together, these factors lead to the concept of the “uniqueness of place” as termed by Beven (2000). Thus, with increasing catchment size it becomes increasingly problematic to treat catchments as lumped entities in models, as these are not suitable for accommodating spatial heterogeneity. In other words, this heterogeneity can in reality result in a variety of parallel processes, characterized by considerably different timescales being simultaneously active. Therefore, lumped representations of catchments frequently fail to adequately represent the dominant features of the observed hydrological response at the catchment scale (e.g. Euser et al., 2015), such as low and high flows at the basin outlet.

Experimentally, the importance of intra-catchment process heterogeneity was for example demonstrated by Seibert et al. (2003a). They showed that groundwater table fluctuations can exhibit considerably distinct dynamics between hillslopes and riparian areas near the stream. Similarly, Detty and McGuire (2010) showed that topographically different landscape elements are characterized by different wetting mechanisms, while others, e.g. McGlynn et al. (2004), Jencso et al. (2009) or Spence et al. (2010), systematically documented distinct response patterns in different parts of catchments.

Lumped applications of hydrological models, such as HBV (Bergström, 1992) or GR4J (Perrin et al., 2003), proved valuable in the past under a wide range of environmental conditions and across a range of scales as they appear to capture the core emergent processes of many hydrological systems (e.g. Refsgaard and Knudsen, 1996; Booij, 2005). Nevertheless, in many cases these models may remain serious over-simplifications of the different combinations of the dominant processes underlying the observed response patterns as argued by, among others, Young (1992), Reichert and Omlin (1997), Perrin et al. (2001), Wagener and Gupta (2005), Gupta et al. (2012), Zehe et al. (2014), Hrachowitz et al. (2014) and Fovet et al. (2015). In addition, the transferability of these simple models to other (ungauged) basins is limited. In the past, distributed models, such as MIKE-SHE (Refsgaard and Storm, 1995) or DHSVM (Wigmosta et al., 1994), but also (semi-)distributed applications of lumped models, were shown to alleviate the issue of over-simplification to a certain extent by accommodating spatial heterogeneity in soil moisture and/or model parameters (e.g. Fenicia et al., 2008; Winsemius et al., 2008; Euser et al., 2015).

However, traditional, conceptual distributed model approaches suffer from several limitations. They are defined

by the grid size of the available data or the size of the defined subcatchments, which are of the order of several dozen square kilometres in most applications (e.g. Booij, 2005; Lindström, 2010). Furthermore, although different model parameters allow for some flexibility in accounting for spatial differences, in a large number of cases the defined processes remain the same among individual model units; that is, the same model architecture is used. This denies the potential for the distinction of different dominant processes belonging to the different parts of the study domain. Even though in some cases triggered by different parameterizations, the importance of this distinction of processes already became apparent in several studies, e.g. Merz and Bárdossy (1998), Zehe et al. (2001), Seibert et al. (2003a), and Das et al. (2008).

Thus, as individual model units are often still represented in a lumped way, sub-grid process heterogeneity in these lumped units is merely reflected by distribution functions or constitutive relationships. For example, distribution functions for maximum unsaturated storage capacities, such as defined in the Xinanjiang model (Zhao, 1992) or the VIC model (Liang et al., 1994), are widely used as a measure of spatial variability of storage capacities on the sub-grid scale. As a second example, the closure problem in the Representative Elementary Watershed approach (Reggiani et al., 1998) addresses the definition of relationships between the spatial variability on the elementary watershed scale and states and fluxes to close the mass and momentum balance equations. Several attempts have been reported to formulate closure relations that allow the accommodation of the spatial heterogeneity within the elementary watershed to varying degrees (e.g. Reggiani and Rientjes, 2005; Zhang and Savenije, 2005; Zhang et al., 2006; Tian et al., 2006; Mou et al., 2008; Vananmetee et al., 2012), but the search for generally applicable adequate closure relations is still ongoing.

The division of the catchment into several functional units (e.g. Knudsen, 1986; Leavesley and Stannard, 1990; Kite and Kouwen, 1992; Kouwen et al., 1993; Flügel, 1995; Reggiani et al., 1998; Winter, 2001; Seibert et al., 2003b; Uhlenbrook et al., 2004; Schmocker-Fackel et al., 2007; Zehe et al., 2014) may offer a way to address these conceptual shortcomings. In spite of the fact that in many cases insufficient data for a detailed delineation of response units are available, it has been recognized (e.g. Beven and Bingley, 1979; Knudsen, 1986) that already topographic data can contain important hydrological information. Starting from that premise, Savenije (2010) argued that through the co-evolution of topography, vegetation and hydrology, different landscape features, such as hillslopes, wetlands or plateaus, do have distinct hydrological functions. This implies that topography alone may contain sufficient information to derive dominant hydrological response units. Distinct response units can therefore be identified based on, for example, the height above the nearest drainage, as a proxy for hydraulic head, and local slope (Rennó et al., 2008; Nobre et al., 2011; Gharari et al., 2011). The different dominant processes char-

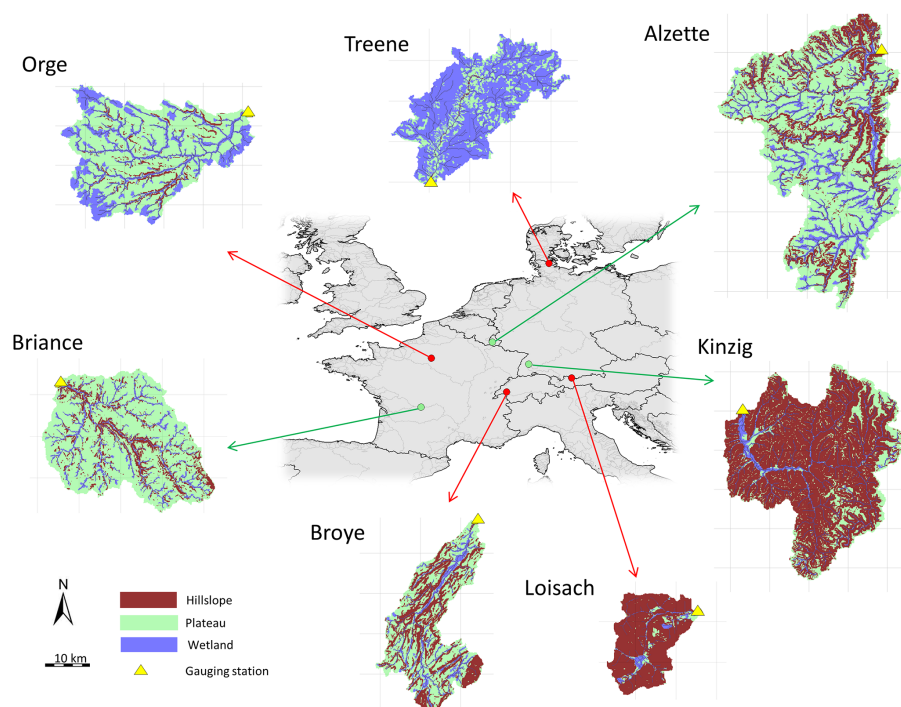


**Figure 1.** The locations of the seven study catchments and their respective landscape classes according to HAND and local slope. Catchments represented by red and green symbols in the context map indicate donor and receiver catchments, respectively, for the transferability analysis. Displayed grids correspond to the modelling grids used in mHM (topo).

acterizing these response units can then be combined into a semi-distributed model with landscape elements acting in parallel. This parsimonious approach to account for process heterogeneity at catchment scale proved highly valuable for improving the skill of otherwise lumped models in reproducing observed system response patterns (e.g. Gao et al., 2014a; Gharari et al., 2014). They further enhance model transferability without the need for empirical transfer functions in widely contrasting environments.

Traditional distributed model applications are characterized by a comparably large parameter space. The typical lack of sufficient model constraints makes it problematic to select meaningful feasible parameter sets. This leads to considerable equifinality (Beven, 1993) and associated problems (cf. Gupta et al., 2008). The need for increased hydrological consistency in models and for more realistic internal model dynamics (i.e. “getting the right answer for the right reasons”; Kirchner, 2006) was recently emphasized as a critical point towards the development of models with higher predictive power (Gupta et al., 2012; Euser et al., 2013; Hrachowitz et al., 2014). This can all be placed in the sense of achieving “the least uncertainty for forecasts” (Kumar, 2011) and needs to be done by more rigorous model testing (e.g. Andréassian et al., 2009; Coron et al., 2012) to meaningfully constrain the feasible model/parameter space.

An efficient method to constrain the parameter space is model regularization (e.g. Tonkin and Doherty, 2005), for ex-

ample by the use of transfer functions (e.g. Abdulla and Lettenmaier, 1997; Hundecha et al., 2004; Pokhrel et al., 2008). Being mathematically equivalent to the concept of regionalization, it was also shown that this is a valuable method to improve spatial model transferability (e.g. Götzinger and Bárdossy, 2007; Samaniego et al., 2010a; Kumar et al., 2013b). However, regularization frequently relies on empirical relationships between catchment characteristics, such as soils, and individual model parameters with little explicit hydrological meaning. In a different approach it was recently shown that semi-quantitative information on catchment functioning based on expert knowledge, often referred to as “soft data” (Seibert and McDonnell, 2002; Van Emmerik et al., 2015), can be highly efficient in constraining models (Kapangaziwiri, 2012; Hughes, 2013; Seibert and McDonnell, 2013; Gao et al., 2014a; Gharari et al., 2014; Hrachowitz et al., 2014).

Considering the potential information embedded in landscapes, the need for simplification and regularization in complex models, and the additional value of expert-based semi-quantitative information, there may be an opportunity to improve distributed hydrological models. To test the value of topography-induced sub-grid process heterogeneity, the principles of landscape-driven modelling (Savenije, 2010) were introduced in the distributed, regularized mesoscale Hydrologic Model (mHM; Samaniego et al., 2010a; Kumar et al., 2013a). It is hypothesized that (1) the incorporation of addi-

tional sub-grid variability on the basis of topography-derived response units improves model internal dynamics and its predictive power, (2) the application of semi-quantitative, expert-knowledge-based model constraints allows the identification of unfeasible parameter sets and thereby reduces model uncertainty, and that (3) the combined use of response units and model constraints improves the spatial transferability of the model.

## 2 Methodology

### 2.1 Study areas

Seven catchments were selected in order to cover a variety of climatological, geographical and geological conditions. The geographical locations as well as the classification of topography-based hydrological response units (i.e. hillslopes, wetlands and plateaus) in the study catchments are shown in Fig. 1. The set of study sites includes catchments with pronounced relief as well as relatively flat and gently sloped catchments. Therefore, some catchments are almost fully dominated by landscapes classified as hillslopes, whereas others contain higher proportions of wetlands. In addition, the climatic variability is considerable, as indicated by the aridity indices ranging from 0.5 to 1.34. Table 1 summarizes the catchment characteristics.

The northern German Treene catchment is a tributary of the Eider River. It is a lowland catchment characterized by sedimentary soils and peat. The land cover is mostly grassland and low vegetation, while only a small percentage is forested or agriculturally used.

The Loisach, Kinzig and Broye catchments are located in mountainous areas, characterized by pronounced relief, steep slopes and the importance of snow. The Loisach and Kinzig catchments are mostly forested, whereas the Broye catchment has mainly open grassland. Sand overlies limestone and other sedimentary bedrock in the Loisach catchment, while the Kinzig catchment is dominated by granite and gneiss series.

The French catchments Orge and Briance are relatively flat with gentle slopes and flat upland areas. Agriculture is the dominant land use, but some forests are also present. The Orge catchment is a tributary of the Seine and contains some of the suburbs of Paris. Thus, it has a significant proportion of urbanized areas (10 %). In the Orge, sandy loam soils have formed on limestone geology, while the Briance is characterized by gravel on gneiss bedrock.

The Alzette catchment in Luxembourg is partly covered by forest (33 % of the catchment area). The rest of the catchment is more open, with grass and shrublands. Limestone, sandstone and schist are the dominant geologic formations, with some clay and loam soil in the upper layers.

Daily discharge time series for all study catchments were obtained from the Global Runoff Data Centre (GRDC). The

daily meteorological data are the gridded E-OBS precipitation and temperature data from the European Climate Assessment and Dataset (ECA&D). The daily potential evaporation was estimated with the Hargreaves equation (Hargreaves, 1985). A summary of the data sources is given in Table 2.

### 2.2 Models

#### 2.2.1 mesoscale Hydrological Model (mHM)

mHM is a distributed, process-based model that uses the cell-wise model architecture shown in Fig. 2 in each grid cell of the modelling domain (Samaniego et al., 2010a; Kumar et al., 2013a). It contains an interception and snow routine to determine the effective precipitation which enters the soil moisture reservoir. For sealed areas the water is directly routed to a fast reservoir. The water infiltrating into the soil is then partitioned into transpiration and percolation to a fast runoff reservoir, i.e. shallow subsurface flow. In addition, this reservoir recharges a lower reservoir that mimics the base-flow component of the runoff. The model has been successfully applied across Germany, Europe and North America (Samaniego et al., 2010a, b, 2013; Kumar et al., 2010, 2013a, b; Livneh et al., 2015; Thober et al., 2015; Rakovec et al., 2015).

#### 2.2.2 Topography-driven mHM (mHMtopo)

To test the value of topography variability-induced process heterogeneity in a distributed model, the concepts of FLEXtopo (Savenije, 2010; Gharari et al., 2011) were applied in mHM. Based on the assumption of distinct hydrological functioning of different landscape elements, sub-grid process heterogeneity was accounted for by a model architecture that allowed an explicit representation of landscape classes identified as dominant in many central European regions: plateaus, hillslopes and wetlands (Savenije, 2010). The landscape classes were defined by the Height Above the Nearest Drainage (Rennó et al., 2008; HAND) and local slope. Following Gharari et al. (2011), areas with a low slope ( $< 11\%$ ) and high HAND ( $> 5\text{ m}$ ) were defined as plateaus, areas with high slope ( $> 11\%$ ) as hillslopes and areas with low slope and low HAND ( $< 5\text{ m}$ ) as wetlands. It is acknowledged that these thresholds remain merely assumptions and may need refinement in other regions. Nevertheless, this refinement is out of the scope of this paper and the used threshold values are assumed to give a reasonable delineation of landscape units in the central European context. The varying proportions of these individual landscape units in each cell in the modelling domain then allow for considerable sub-grid process heterogeneity in the distributed model, as the total outflow of a cell is then the area-weighted average of the outflows from the individual landscape units. The assumptions behind the conceptualizations of the three landscape classes are briefly sum-

**Table 1.** Overview of the catchments.

Catchment	Country	Area (km <sup>2</sup> )	Elevation (mMSL)	Runoff (mm yr <sup>-1</sup> )	Aridity index (EP / P) (–)	Calibration period	Validation period
Alzette	Luxembourg	1172	194–545	286	0.90	01/01/1978–31/12/1980	01/01/1983–31/12/1987
Briance	France	604	211–719	377	0.88	01/01/1982–01/07/1993	02/07/1993–31/12/2004
Broye	Switzerland	396	391–1494	648	0.71	01/01/1995–02/07/1987	03/07/1987–31/12/2009
Kinzig	Germany	955	172–1084	759	0.67	01/01/1951–31/12/1971	01/01/1971–31/12/1990
Loisach	Germany	243	716–2783	960	0.50	01/01/1976–31/12/1988	01/01/1989–31/12/2001
Orge	France	965	38–196	130	1.34	01/01/1968–01/07/1986	02/07/1986–31/12/2004
Treene	Germany	481	–1–80	428	0.75	01/01/1974–01/07/1989	02/07/1989–31/12/2004

**Table 2.** Overview of the used data.

Data type	Product	Source	Reference
Soil	HWSD	<a href="http://webarchive.iiasa.ac.at/Research/LUC/">http://webarchive.iiasa.ac.at/Research/LUC/</a>	FAO/IIASA/ISRIC/ISSCAS/JRC (2012)
Topography	SRTM	<a href="http://hydrosheds.cr.usgs.gov/index.php">http://hydrosheds.cr.usgs.gov/index.php</a>	Lehner et al. (2008)
Discharge	GRDC	<a href="http://www.bafg.de/GRDC/EN/">http://www.bafg.de/GRDC/EN/</a>	The Global Runoff Data Centre, 56002 Koblenz, Germany
Precipitation	E-OBS	<a href="http://eca.knmi.nl/download/ensembles/ensembles.php">http://eca.knmi.nl/download/ensembles/ensembles.php</a>	Haylock et al. (2008)
Land cover	Globcover	<a href="http://due.esrin.esa.int/page_globcover.php">http://due.esrin.esa.int/page_globcover.php</a>	Arino et al. (2009)

marized in the following. For details the reader is referred to Savenije (2010) and Gharari et al. (2014).

The different model structures for these three classes run in parallel, connected by a common groundwater reservoir for each modelling cell, as can be seen in Fig. 3. The primary hydrological functions of plateau landscapes are, in the absence of significant topographic gradients, mainly groundwater recharge and evaporation/transpiration, i.e. vertical fluxes. To account for potential agricultural drainage systems, a fast reservoir is included in the plateau model structure. Hill-slopes are assumed to be the dominant source of storm flow and efficiently contribute to storm runoff through storage excess shallow subsurface flow, e.g. preferential flow, here conceptualized by a fast reservoir. The wetland landscape is assumed to interact more strongly with the groundwater. Thus, capillary rise (Cr in Fig. 3) is included to interact with the soil moisture reservoir. The wetlands are assumed to have shallow groundwater tables and associated low storage capacities. Therefore, saturation excess overland flow, represented by a fast responding reservoir, and evaporative processes are assumed to be dominant in this landscape unit.

Throughout the rest of this paper, the two models will be referred to as mHM and mHMtopo to distinguish between the original mHM and the topography-guided set-up, respectively.

## 2.3 Model regionalization, regularization and prior constraints

Reducing the feasible model parameter space is strongly associated with a reduction in parameter equifinality and model uncertainty, and can be achieved by imposing constraints on

the model, for example by regularization. Only parameter sets that can satisfy these constraints will then be retained as feasible, while others will be discarded. A method that uses empirical transfer functions relating parameter values to physical catchment characteristics is also a powerful tool to regionalize models.

### 2.3.1 Multiscale parameter regionalization

The multiscale parameter regionalization (MPR) is the key feature of mHM (Samaniego et al., 2010a; Kumar et al., 2013a). The global parameters in mHM are, in contrast to typical models, not hydrologic model parameters (e.g. soil porosity). Instead, the global parameters define the functional relationship between the individual hydrologic model parameters and physical catchment characteristics at the spatial resolution of the data of the latter. A set of global parameters is obtained by simultaneously calibrating on multiple catchments. This set of global parameters can then be transferred to other catchments where the same data of physical catchment characteristics are available without the need for further calibration.

Thus, the functional relationships are used in a first step to estimate model parameters on the spatial resolution of the input data. As depicted in Fig. 4, as an example, the leaf area index is linearly linked through global parameters with the hydrologic model parameter of interception capacity ( $I_{\max}$ ). Assuming the relationships are adequate, the use of additional data of preferably multiple, distinct catchments may increase the general validity of these relationships and, thus, the global parameters.

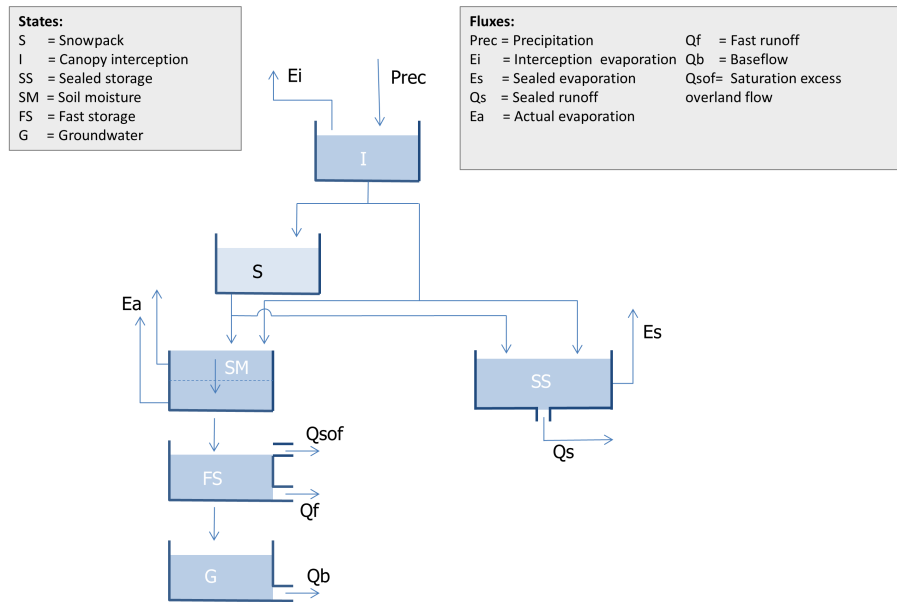


**Figure 2.** The original mHM model structure. The effective precipitation is determined by an interception (I) and a snow routine (S). Afterwards, the effective precipitation enters a soil moisture reservoir (SM) or is directly routed to a fast reservoir that accounts for sealed areas (SS). The water in the soil moisture reservoir either transpires or percolates further down to a fast runoff reservoir (FS), i.e. shallow subsurface flow. Eventually, the baseflow component of the runoff is obtained from a slow groundwater reservoir (G).

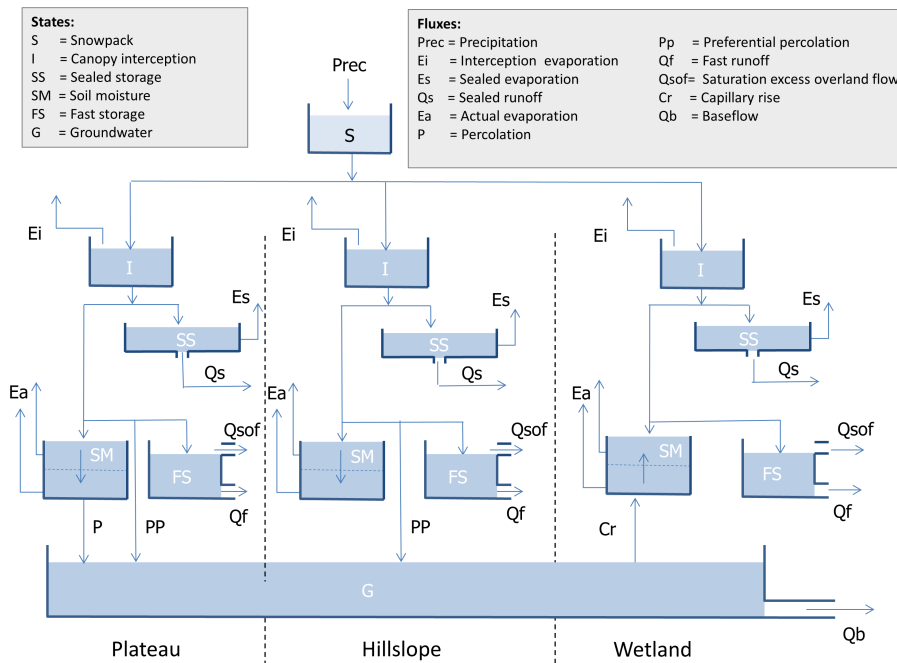


**Figure 3.** The mHMtopo model structure with different configurations of states and fluxes for landscape classes plateau, hillslope, and wetland, which are based on topography. First, a shared snow module (S) divides the effective precipitation over the landscape classes. The three classes all have an interception module (I), a fast reservoir accounting for sealed areas (SS), a soil moisture routine (SM) and a fast reservoir (FS). The plateau landscapes are assumed to feed the groundwater through percolation (P) from the soil moisture and preferential percolation (PP). The steeper hillslope areas are assumed to merely feed the groundwater through preferential percolation (PP), whereas the wetlands receive water through capillary rise (Cr). The baseflow is determined by a shared groundwater reservoir.



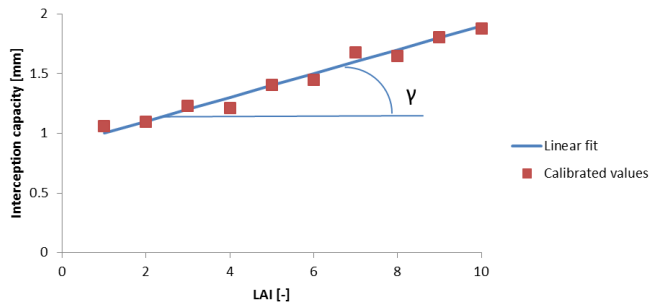


**Figure 4.** Function relationship between leaf area index (LAI) and the hydrologic parameter interception capacity ( $I_{0,\max}$ ) defined by the global parameter  $\gamma$ , based on fictional data for illustration.

Figure 5 depicts the application of the MPR technique to gridded data. The obtained hydrologic parameters, determined by the functional relationships, still have a resolution equal to the input data. In most cases, this is not equal to the modelling resolution. Therefore, a second step in the MPR is the upscaling of hydrologic parameters to the modelling resolution (in this study,  $8\text{ km} \times 8\text{ km}$ ). This upscaling can either be achieved by using the harmonic mean, arithmetic mean or maximum value over the cells within the modelled grid cell. The choice of the upscaling method strongly depends on the parameter under consideration. The reader is referred to Samaniego et al. (2010a) and Kumar et al. (2013a) for details about the transfer functions and upscaling methods.

The MPR technique has been adjusted in two ways for use in mHMtopo. The regionalization functions were used for the three individual landscape units, whereby each landscape unit was assigned its own global parameters. In other words, the functional relations between physical catchment characteristics (e.g. soil, slope) and hydrologic parameters were kept the same, but the global parameters of these relations differ between landscape units. For example, the LAI is now individually linked with three global parameters for wetland, hillslopes and plateaus, respectively, to obtain three hydrologic parameters for interception capacity ( $I_{\max,\text{plateau}}$ ,  $I_{\max,\text{hillslope}}$ ,  $I_{\max,\text{wetland}}$ ); see Fig. 5.

The second change was in the upscaling. Instead of scaling up over all high-resolution cells within a modelling unit, the upscaling was carried out for each landscape class within a modelling unit. The upscale operators for mHMtopo were adopted from similar parameters in mHM. For example, the upscaling of the interception capacities was done by the arithmetic mean, similar to that of the upscaling of interception capacities used in the original mHM (see Fig. 5).

### 2.3.2 Expert-knowledge-based prior constraints

In addition to MPR, we tested the value of semi-quantitative, relational prior parameter and process constraints (Gharari et al., 2014; Hrachowitz et al., 2014) for the robustness of process representation and model transferability. In other words,

only global parameter sets that satisfied these parameter and process constraints during calibration were accepted as feasible and used in validation and post-calibration evaluation.

Specifically, constraints for the long-term mean annual runoff coefficients were formulated to ensure plausible water partitioning between evaporation and runoff. The limits were chosen as the maximum and minimum annual runoff coefficients  $C_{R\max}$  and  $C_{R\min}$  occurring over the calibration time period. The months May–September were defined as a high flow period, whereas low flows were assumed to occur over the months October–April. Only for the Loisch catchment were these periods switched, as this catchment has high flows starting in spring due to snowmelt. The following three constraints were used: one taking into account the whole time series ( $C_R$ ) as well as one for the high flow period ( $C_{R\text{high}}$ ), and one for the low flow period ( $C_{R\text{low}}$ ) to improve the seasonal variation of the model response behaviours.

$$C_{R\min} < C_{R\text{modelled}} < C_{R\max} \quad (1)$$

$$C_{R\text{high},\min} < C_{R\text{high},\text{modelled}} < C_{R\text{high},\max} \quad (2)$$

$$C_{R\text{low},\min} < C_{R\text{low},\text{modelled}} < C_{R\text{low},\max} \quad (3)$$

The topography driven model, mHMtopo, is also constrained on soil moisture storage capacity ( $S_M$ ). On hillslopes and plateaus the groundwater table can be assumed to be deeper than in wetlands, and root systems generate a larger dynamic part of the unsaturated zone (cf. Gao et al., 2014b). Therefore, they are conceptualized to have a higher water storage capacity than wetlands, which are typically characterized by a very shallow groundwater table. This reasoning reflects not only the variable contribution area theory of Dunne (1975) and the concept of a topographic wetness index (Beven, 1979), but also results from experimental studies, e.g. Seibert et al. (2003a). Thus, two additional constraints were used for mHMtopo:

$$S_{M,\text{plateau}} > S_{M,\text{wetland}}, \quad (4)$$

$$S_{M,\text{hillslope}} > S_{M,\text{wetland}}. \quad (5)$$

## 2.4 Experiment set-up

### 2.4.1 Calibrated model comparison

The two models, i.e. mHM and mHMtopo, were calibrated for each catchment with a random Monte Carlo sampling approach based on 100 000 realizations and a multi-objective strategy using four objective functions: the Nash–Sutcliffe efficiency of flow ( $E_{NS,Q}$ ), the Nash–Sutcliffe efficiency of the logarithm of flow ( $E_{NS,\log Q}$ ), the volume error of flow ( $E_{V,Q}$ ) and the Nash–Sutcliffe efficiency of the logarithm of the flow duration curve ( $E_{NS,FDC}$ ). The four objective functions were chosen as they characterize different aspects of the flow response. Therefore, these objective functions are expected to provide hydrologically relatively consistent and robust parameter sets.

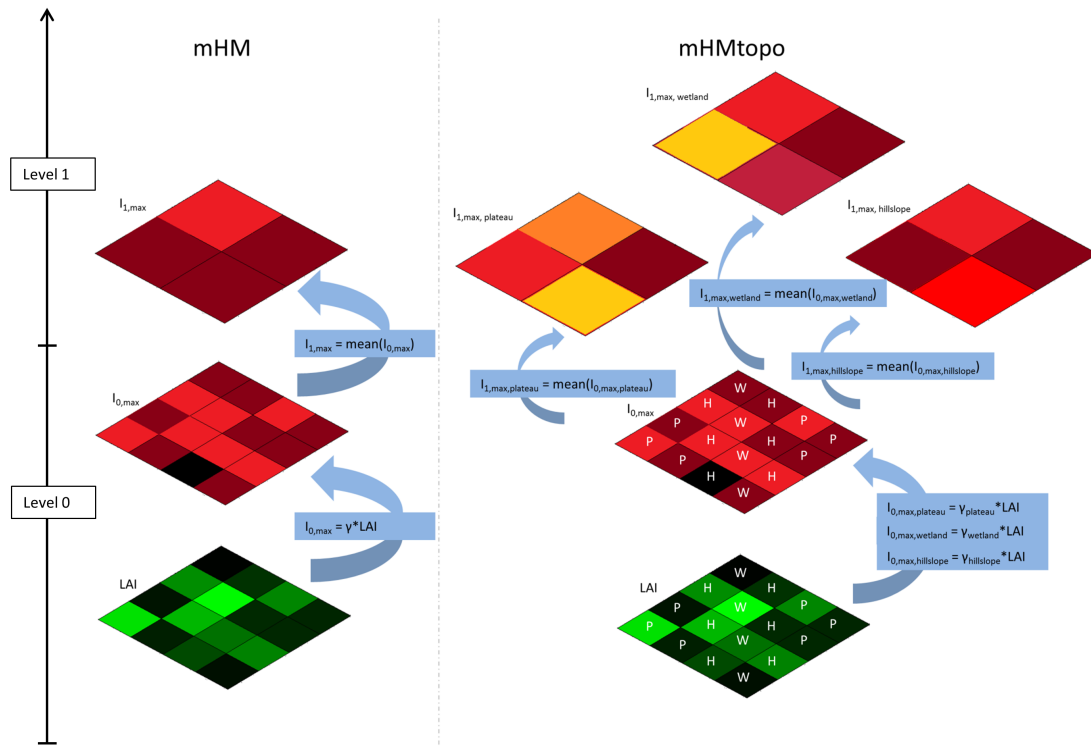


**Figure 5.** Schematic representation of the original MPR (left) and the adjusted MPR (right) for the maximum interception capacity ( $I_{1,max}$ ). On the input level 0, the leaf area index (LAI) is linked through the global, generally valid, parameter  $\gamma$  with  $I_{0,max}$ . In a last step, the mean is used for upscaling, yielding  $I_{1,max}$  at the modelling resolution. For mHMtopo, the functional relations are the same, but plateau (P), hillslope (H) and wetland (W) have their own global parameters  $\gamma$ . The upscaling is subsequently carried out over each landscape class within each grid cell. This leads to the interception capacities of plateau, hillslope and wetland ( $I_{1,max,plateau}$ ,  $I_{1,max,hillslope}$  and  $I_{1,max,wetland}$ ).

This calibration strategy was preferred over other calibration schemes, such as the Dynamically Dimensioned Search algorithm (Tolson and Shoemaker, 2007; DDS) or the Shuffled Complex Evolution method (Duan et al., 1992; SCE), to obtain a set of feasible parameter solutions instead of one optimal solution. As the mathematically optimal solution may not be the hydrologically most adequate solution (cf. Beven, 2006; Kirchner, 2006; Andréassian et al., 2012), this is necessary to make a robust assessment of the model's abilities. Therefore, all parameter sets that satisfy all model constraints and that are contained in the parameter space spanned by the four-dimensional Pareto front formed by  $E_{NS,Q}$ ,  $E_{NS,\log Q}$ ,  $E_{V,Q}$  and  $E_{NS,FDC}$  were considered to be feasible solutions and used for post-calibration evaluation. Considering all feasible solutions to be equally likely, the model uncertainty intervals are represented by the envelope of all feasible solutions.

#### 2.4.2 Post-calibration model evaluation

The models' skill in reproducing a variety of observed hydrological signatures, i.e. emergent properties of a system (Eder et al., 2003), was evaluated after calibration to test the hydrological consistency of the models. Hydrological signatures

allow evaluation of the consistency and reliability of hydrologic simulations by taking more features of the hydrological response into account than only the flow time series. In a nutshell, the more signatures a model can simultaneously reproduce in addition to the hydrograph, the more plausible it is that a model (and its parameters) will adequately reflect the underlying dominant system processes (e.g. Euser et al., 2013). All signatures used in this study were selected based on earlier work (e.g. Sawicz et al., 2011; Euser et al., 2013) and are summarized in Table 3.

Although not fully independent of each other, the signatures, such as the peak flow distribution, the rising limb density and the autocorrelation function of flow, contain information on different aspects of the hydrologic response. The Nash–Sutcliffe efficiency  $S_{NS}$  was used as a performance metric to assess the model skill in case of multi-value signatures such as the peak flow distribution or the autocorrelation function. In contrast, the relative error  $S_{RE}$  was used for single-valued signatures, such as the mean annual runoff. The Euclidian distance  $D_E$  to the “perfect model” was used as an overall measure of a model's ability to reproduce all



**Table 3.** Overview of the used signatures.

Signature	Description	Reference
$Q_{MA}$	Mean annual runoff	
AC	One-day autocorrelation coefficient	Montanari and Toth (2007)
AC <sub>low</sub>	One-day autocorrelation low flow period	Euser et al. (2013)
AC <sub>high</sub>	One-day autocorrelation high flow period	Euser et al. (2013)
RLD	Rising limb density	Shamir et al. (2005)
DLD	Declining limb density	Shamir et al. (2005)
$Q_5$	Flow exceeded in 5 % of the time	Jothityangkoon et al. (2001)
$Q_{50}$	Flow exceeded in 50 % of the time	Jothityangkoon et al. (2001)
$Q_{95}$	Flow exceeded in 95 % of the time	Jothityangkoon et al. (2001)
$Q_{5,low}$	Flow exceeded in 5 % of the low flow time	Yilmaz et al. (2008)
$Q_{50,low}$	Flow exceeded in 50 % of the low flow time	Yilmaz et al. (2008)
$Q_{95,low}$	Flow exceeded in 95 % of the low flow time	Yilmaz et al. (2008)
$Q_{5,high}$	Flow exceeded in 5 % of the high flow time	Yilmaz et al. (2008)
$Q_{50,high}$	Flow exceeded in 50 % of the high flow time	Yilmaz et al. (2008)
$Q_{95,high}$	Flow exceeded in 95 % of the high flow time	Yilmaz et al. (2008)
Peaks	Peak distribution	Euser et al. (2013)
Peaks <sub>low</sub>	Peak distribution low flow period	Euser et al. (2013)
Peaks <sub>high</sub>	Peak distribution high flow period	Euser et al. (2013)
$Q_{peak,10}$	Flow exceeded in 10 % of the peaks	
$Q_{peak,50}$	Flow exceeded in 50 % of the peaks	
$Q_{low,peak,10}$	Flow exceeded in 10 % of the low flow peaks	
$Q_{low,peak,50}$	Flow exceeded in 10 % of the low flow peaks	
$Q_{high,peak,10}$	Flow exceeded in 10 % of the high flow peaks	
$Q_{high,peak,50}$	Flow exceeded in 50 % of the high flow peaks	
AC <sub>serie</sub>	Autocorrelation series (200-day lag time)	Montanari and Toth (2007)

signatures under consideration (e.g. Schoups et al., 2005):

$$D_E = \sqrt{(1 - S_{NS,1})^2 + (1 - S_{NS,2})^2 \dots + (1 - S_{NS,n})^2} + S_{RE,1}^2 + S_{RE,2}^2 \dots + S_{RE,m}^2, \quad (6)$$

with  $S_{NS,i}$  the performance metric of  $n$  multi-valued signatures, and  $S_{RE,j}$  for the  $m$  single-valued signatures.

From calibration, a set of feasible parameter sets was obtained for each tested model, which inevitably resulted in varying skills to reproduce the system signatures for the individual parameter sets. The probability that one model will outperform another for a specific signature was computed to objectively quantify the differences between these distributions and to allow an overall assessment of which of the tested models exhibits a higher ability to reproduce the individual signatures. As estimates of the empirical performance distributions are available based on all parameter sets retained as feasible, the probability of improvement  $P_{1,S}$  can be readily obtained from

$$P_{1,S} = P(S_1 > S_2) = \sum_{i=1}^n P(S_1 > S_2 | S_1 = r_i) P(S_1 = r_i), \quad (7)$$

where  $S_1$  and  $S_2$  are the signature performance metrics of the two models,  $r_i$  a realization from the  $S_1$  distribution and  $n$  the total number of realizations of the  $S_1$  distribution. Thus,

a probability of 0.5 indicates that in 50 % of the cases model 1 and in 50 % of the cases model 2 performs better; that is, no preference for a model can be identified. In contrast, for  $P_{1,S} > 0.5$  it is more likely that model 1 outperforms model 2 with respect to the signature under consideration, and vice versa for  $P_{1,S} < 0.5$ .

In an additional analysis, the ranked probability score  $S_{RP}$  (Wilks, 2011) was calculated as a measure of the magnitude of improvement. For details, please see the description and Fig. S1 in the Supplement.

### 2.4.3 Comparison of model transferability

The mHM hydrologic model has previously been shown to have a considerable ability to reproduce the hydrograph when transferring global parameters from calibration catchments to other regions without further recalibration (Samaniego et al., 2010a, b; Kumar et al., 2013a, b; Rakovec et al., 2015). Therefore, it was tested whether the addition of topography-driven sub-grid process heterogeneity and the use of prior constraints in mHM have the potential to further improve this transferability. Four catchments were used as donor catchments to obtain one set of global parameters via simultaneous calibration. The Orge, Treene, Broeye and Loisch were chosen as donor catchments as they are geographically far from each other, introducing a wide range

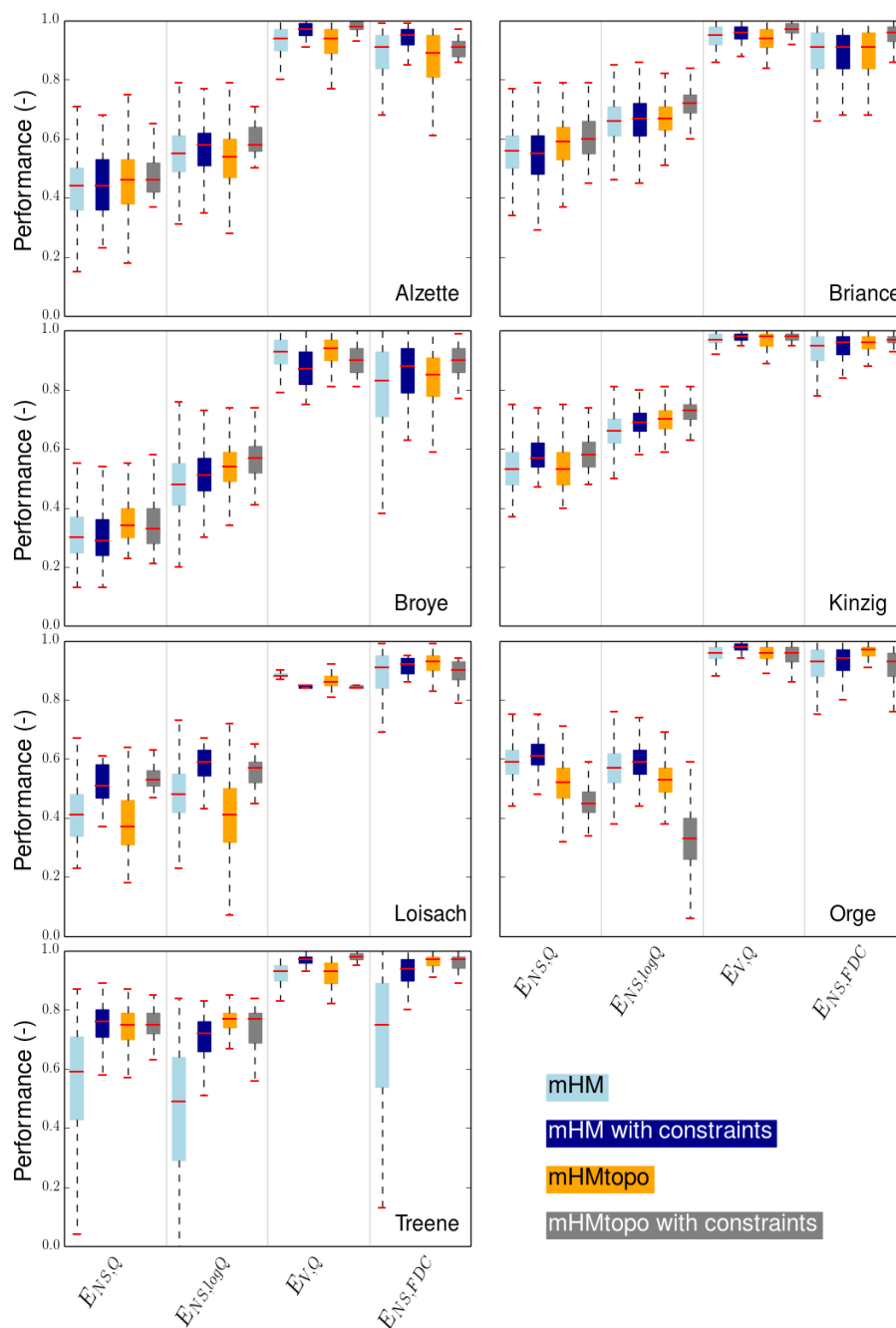


**Figure 6.** Nash–Sutcliffe efficiency ( $E_{NS,Q}$ ), log Nash–Sutcliffe efficiency ( $E_{NS,\log Q}$ ), volume error ( $E_{V,Q}$ ) and log Nash–Sutcliffe efficiency of the flow duration curve ( $E_{NS,FDC}$ ) for the seven catchments in the validation periods. The optimal value for all four criteria is 1, whereas 0 is regarded as having a low performance. The boxplots are formed by the Pareto space spanned by the four objective functions.

in climate and catchment characteristics. The receiver catchments are the three remaining catchments of Alzette, Briance and Kinzig.

This was carried out with the same calibration strategy as for the individual catchment calibrations. However, the four objective functions  $E_{NS,Q}$ ,  $E_{NS,\log Q}$ ,  $E_{V,Q}$  and  $E_{NS,FDC}$  were now averaged over the catchments. This led to global

parameters that account for the performance in all donor catchments. These averaged values were then used to determine the Pareto space of feasible parameter sets again. The feasible solutions were transferred and used in the three remaining receiver catchments without any further recalibration. We fully acknowledge that this analysis can only give a sense of what is possible and that a full bootstrap proce-

ture and the analysis of more catchments would have allowed a more robust interpretation of the results, but this was unfeasible given the computational demands of the calibration procedure. The calibrations were carried out on the EVE high-performance compute cluster of the UFZ Leipzig which has 84 compute nodes with dual-socket Intel Xeon X5650 processors with 64 GB RAM as well as 65 compute nodes with dual-socket Intel Xeon E5-2670 processors. Nevertheless, the used calibration strategy needed run times of about 2 weeks per catchment on multiple EVE cores, depending on catchment sizes and lengths of time series.

### 3 Results and discussion

#### 3.1 Calibrated model comparison

The two different models mHM and mHMtopo, both with and without additional prior constraints, exhibited adequate and similar calibration performances with respect to all four calibration objective functions (see Fig. S2 in the Supplement). For the validation period it was found that performance generally improved by applying prior constraints and by allowing for topography-guided sub-grid process heterogeneity. This can be seen from Fig. 6, where mHM with constraints (dark blue) compared with mHM (light blue) generally has an increased performance. The same is true for mHMtopo with constraints (orange) compared with unconstrained mHMtopo (grey). At the same time, it can be noted from Fig. 6 that the addition of topography-guided sub-grid variability leads to a general moderate improvement in performance. Overall, the introduction of constraints to mHM resulted in an average improvement of 13 % with regard to the Euclidian distance  $D_E$  for the objective function values in validation. In addition, unconstrained and constrained mHMtopo exhibited an average increase of 8 and 11 %, respectively, for the Euclidian distance  $D_E$  compared to the original mHM.

##### 3.1.1 Effect of sub-grid heterogeneity

The incorporation of sub-grid process heterogeneity did not show a clear pattern of improvements or deterioration. Some catchments experienced performance increases in terms of the used objective functions during validation, like the Briance catchment. The predictive performance of others, also in terms of the used objective functions, slightly decreased, such as the Orge catchment. These findings support the results of Orth et al. (2015), who also found that added complexity, here in the sense of an increased number of processes and parameters, does not necessarily lead to model improvements. However, these findings are not in line with some other previous work (e.g. Gharari et al., 2013; Gao et al., 2014a; Euser et al., 2015), which all concluded that parallel model structures increased model performance. It can be argued that for mHM, whose global parameters are to a

certain extent already functions of landscape variability, additional sub-grid process heterogeneity is not warranted by the available data and can thus not be resolved by the model when there are relatively few contrasts in the landscape.

The Treene catchment benefits most from the addition of topography-guided sub-grid heterogeneity (Fig. 6). Here, a large area is classified as wetland, where the soil moisture is fed by groundwater through capillary rise. This process is fully absent in the original mHM structure, but is an important process in this relatively flat and humid catchment, dominated by peaty soils. These findings also correspond to conclusions by Schmalz (2008, 2009), who applied the SWAT model in the same catchment and noticed that shallow groundwater and soil moisture parameters are very sensitive to low flows. It may also be noted that for mHMtopo the bandwidth of the feasible solutions around the observed hydrograph is considerably reduced as compared to mHM, in particular during low flows. Figure 7 shows that in the months April–July the uncertainty range is significantly larger for mHM than for mHMtopo. In addition, it is interesting to note that the lower bound of flow in mHM reaches towards  $0 \text{ mm d}^{-1}$  in July, whereas mHMtopo still maintains a flow.

In contrast, it can be noticed from Fig. 6 that the consideration of sub-grid process heterogeneity causes a decrease in performance compared to the original mHM in the Orge catchment. This catchment has a relatively large urban area of about 10 %. In addition, these areas are rather densely populated and the river contains several human-made adjustments such as weirs (Le Pape, 2012). Therefore, it is more markedly influenced by anthropogenic disturbances, which are likely not adequately reflected in either mHM or mHMtopo. This results in a situation where the more parsimonious mHM is likely to provide a representation of process dynamics that more closely reflects those observed. The higher number of parameters in mHMtopo provides not only more freedom for adequate system representations, but also for misrepresentations. Thus, after an adequate calibration a larger part of the “feasible” mHMtopo parameter sets fails to mimic the observed response patterns in the validation period compared to mHM. In addition, it can also be observed from the hydrographs that the Orge is a fast responding catchment with very spiky flow peaks (Fig. 8). The addition of more storage reservoirs in mHMtopo delays the signal more than the simpler model structure, leading to a reduced ability to reproduce this spiky behaviour.

##### 3.1.2 Effect of constraints

The applied prior process and parameter constraints, in agreement with Gharari et al. (2014b) and Hrachowitz et al. (2014), helped to increase model performance (Fig. 6) and to reduce model uncertainty (Figs. 7, 8, 9) by identifying and discarding a considerable number of model solutions that did not satisfy these constraints. Rather, these discarded solu-

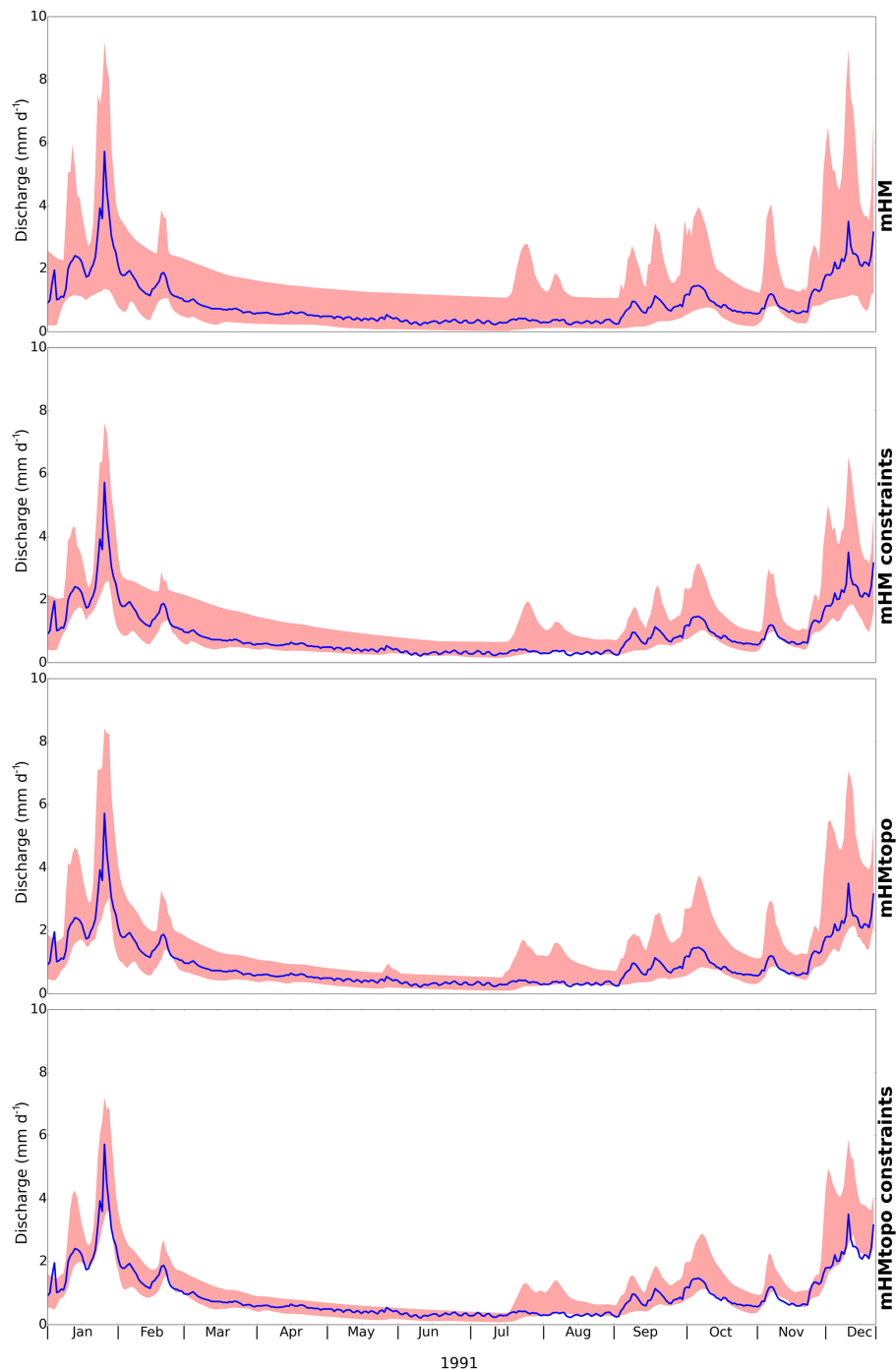


**Figure 7.** Hydrographs for the Treene catchment, with, respectively, the hydrographs for mHM, mHM with constraints, mHMtopo and mHMtopo with constraints. The red shaded areas represent the envelope spanned by all feasible solutions, whereas the blue line corresponds to observed values.

tions violated observed partitioning patterns between runoff and evaporative fluxes and conflicted with our understanding of how the catchments respond. Being merely manifestations of a successful mathematical optimization process, rather than plausible representations of system-internal re-

sponse dynamics, the discarded solutions underline how deceptive adequate calibration results can be and how a successful identification can result in reduced predictive uncertainty. It must be noted that the effect is strong in the chosen calibration strategy, as a large set also containing less op-

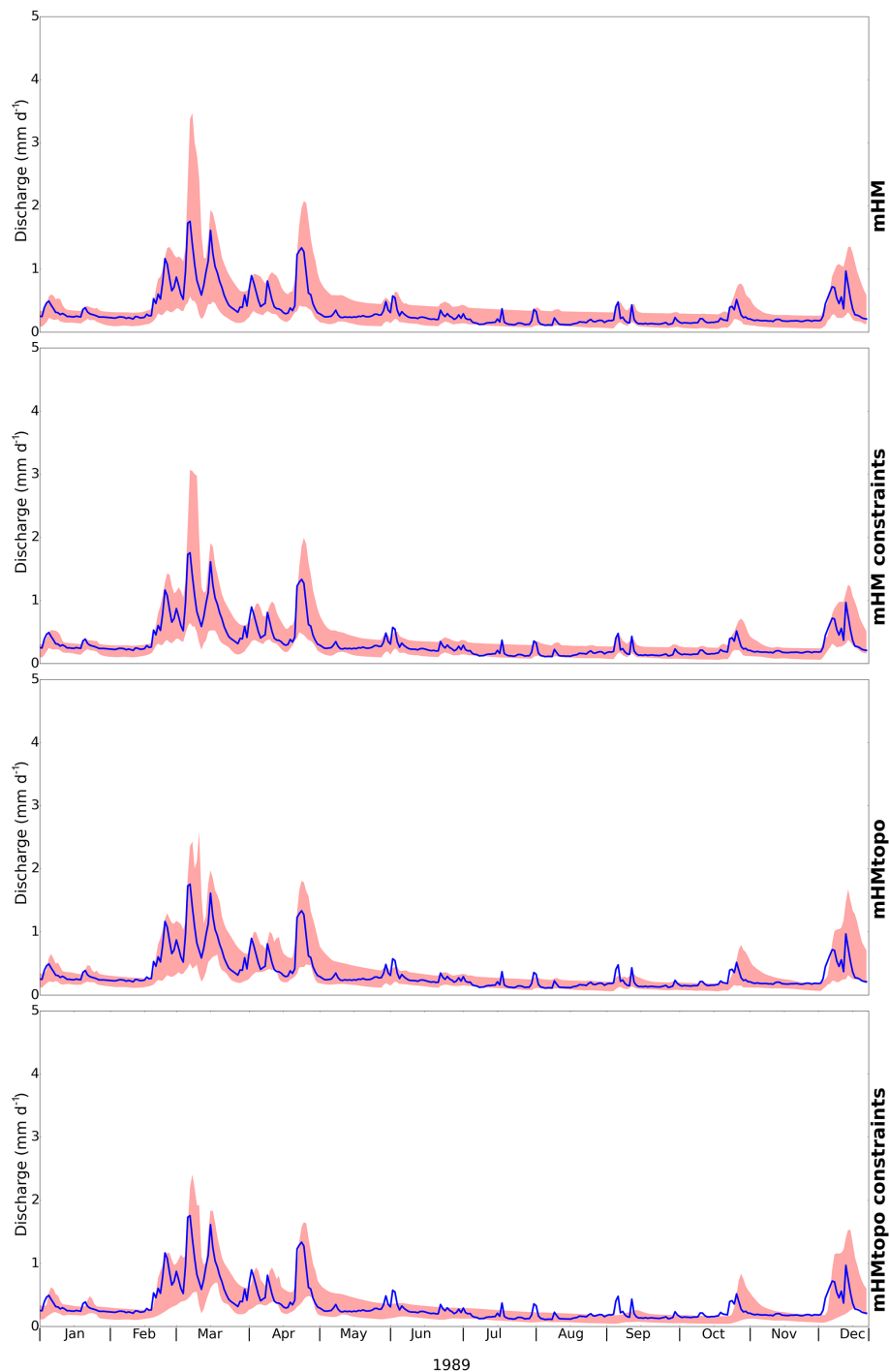


**Figure 8.** Hydrographs for the Orge catchment, with, respectively, the hydrographs for mHM, mHM with constraints, mHMtopo and mHMtopo with constraints. The red shaded areas represent the envelope spanned by all feasible solutions, whereas the blue line corresponds to observed values.

timal solutions is maintained as feasible, but it has already been shown that other calibration procedures may also benefit from additional constraints (Gharari et al., 2014b). This is true as constraints limit the parameter search space with feasible solutions that the algorithm has to explore. In addition,

while traditional calibration procedures may converge to a mathematically optimal fit, additional constraints can test the found solutions for hydrological consistency.

More specifically, the Loisach catchment benefits considerably from the applied constraints. This can be explained by

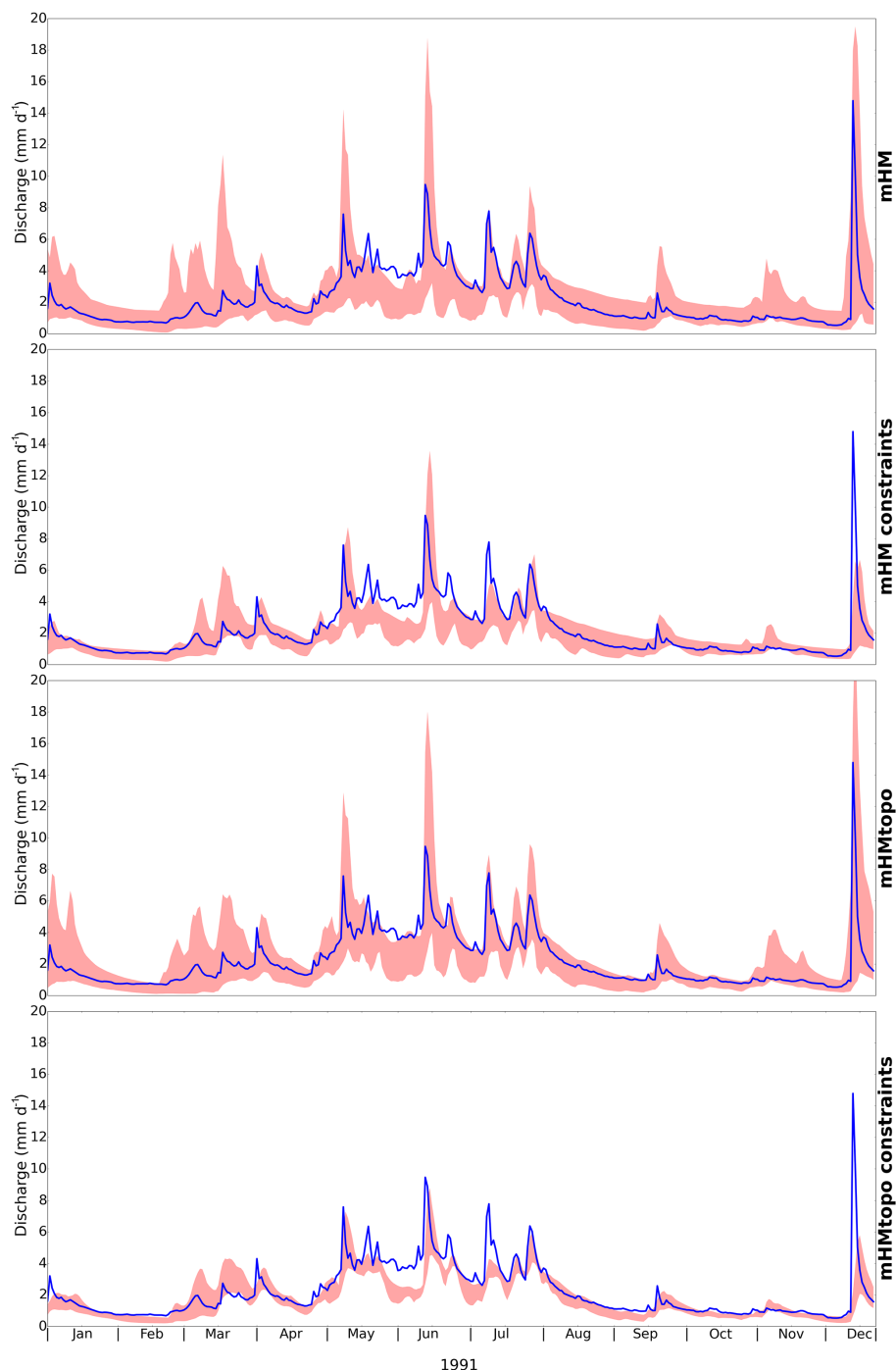


**Figure 9.** Hydrographs for the Loisach catchment, with, respectively, the hydrographs for mHM, mHM with constraints, mHMtopo and mHMtopo with constraints. The red shaded areas represent the envelope spanned by all feasible solutions, whereas the blue line corresponds to observed values.

the fact that this is one of the few catchments in this study where snowmelt plays an important role. For this catchment, temperature is in phase with the high flows, which causes difficulties in water partitioning in the unconstrained models, resulting in evaporative fluxes being too high and stream-

flow being too low. A similar observation for the Loisach was found by Muerth et al. (2013). Even though forced by an ensemble of climate models, the winter flows were too high for an ensemble of hydrological models run for this catchment. Hence, the application of runoff constraints for high



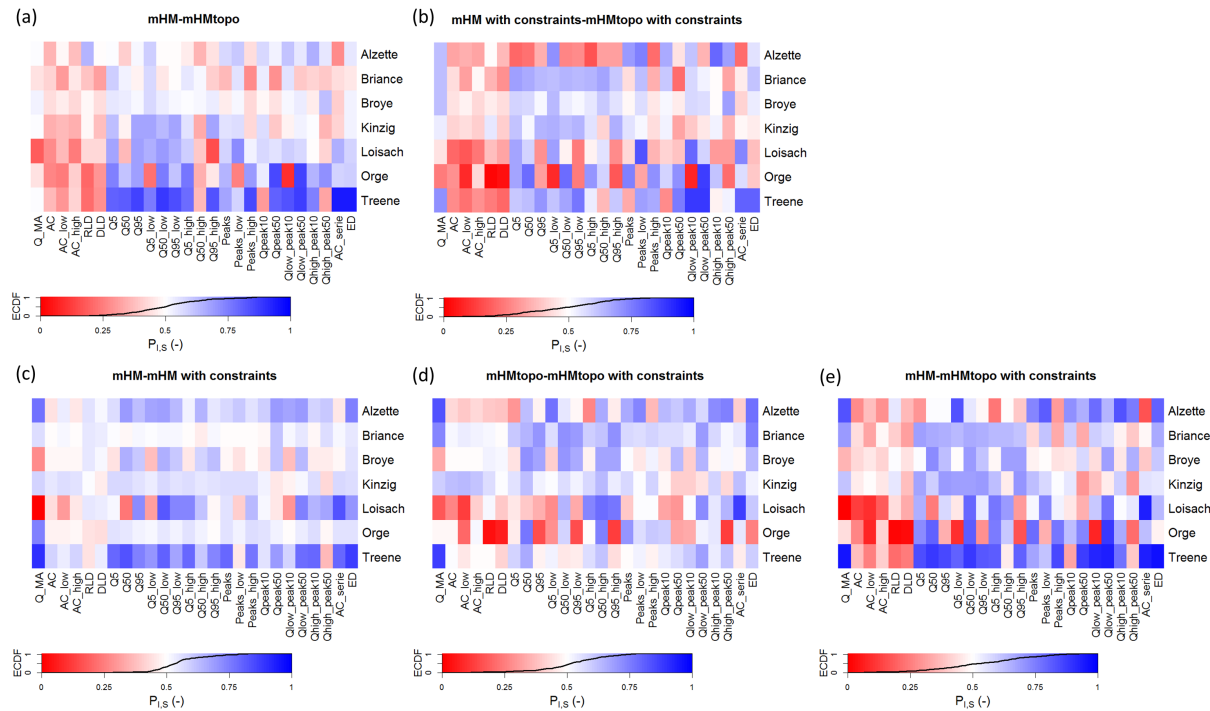


**Figure 10.** Probabilities of improvements  $P_{I,S}$  between (a) mHM and mHMtopo without constraints and (b) with constraints, (c) mHM with and without constraints, (d) mHMtopo with and without constraints and (e) the base case mHM with the constrained mHMtopo case. The colours are linearly related to the probability of improvement between 0 (dark red; e.g. the probability of mHMtopo outperforming mHM is 0), 0.5 (white; i.e. models are statistically equivalent) and 1 (dark blue; e.g. the probability of mHMtopo outperforming mHM is 1). An empirical cumulative distribution function (ECDF) based on all probabilities of improvement has been added to assess the distribution of these probabilities.

and low flow periods led to a considerable improvement in the model's internal dynamics. This is supported by visual inspection of the hydrographs (Fig. 9): both, the constraints for mHM and mHMtopo, cause a significant reduction in the uncertainty bandwidth of the modelled hydrograph, particularly during high flow periods. The unconstrained models have a relatively low lower boundary during high flows, whereas the boundaries in the constrained cases stay much closer to the observed values. Nevertheless, it must also be noted that both models tend to slightly underestimate the flows in the high flow period.

### 3.1.3 Effect of constraints and sub-grid heterogeneity

Comparing the base case of the unconstrained mHM with the most complex constrained mHMtopo (Fig. 6) shows that in most cases improvements are observed. As stated before, compared with the unconstrained mHM, the constrained mHMtopo exhibited an average increase of 8 and 11 %, respectively, for the Euclidian distance  $D_E$ . In most cases, a narrowing of the distribution of objective function values can be observed. For example, the Alzette shows a considerable reduction in the bandwidths of the objective function values. Several catchments also show a substantial shift towards

more optimal solutions. The Loisach catchment, as an example, is one of the catchments where this can be observed.

The only catchment that shows neither a decrease in bandwidth nor a shift upward for any of the four objective function value distributions is the Orge catchment. Moreover, it shows a strong deterioration in terms of objective functions when constraints and sub-grid heterogeneity are added. The processes included in mHMtopo may not be suitable in this case, as the human influences are strong in this catchment. Thus, as stated before, the more parsimonious mHM better reflects the observed dynamics in this catchment in terms of the objective functions.

### 3.2 Signature comparison

The two models mHM and mHMtopo, both unconstrained and constrained, were compared for their ability to reproduce a wide range of hydrological signatures (Table 3). This comparison is based on the probabilities of improvement  $P_{I,S}$  (Fig. 10 and Eq. 6), but similar results were obtained with the ranked probability score  $S_{RP}$ . The results of  $S_{RP}$  can be found in the supplementary material in Figs. S3 and S4. Overall, the introduction of constraints to mHM led to an average improvement of 13 % in terms of the Euclidian distance  $D_E$ .

The introduction of topography had a similar effect, with an average improvement of 13 % for  $D_E$ . The constrained mHMtopo case even experienced an average improvement of 19 %.

### 3.2.1 Effect of sub-grid heterogeneity

Similar to the model performance in the validation periods, no clear pattern emerges for the different models' ability to reproduce the system signatures. The Euclidean distance metric, depicted in the last column of Fig. 10a, illustrates that the consideration of sub-grid process heterogeneity in mHMtopo leads to a slight overall improvement compared to mHM. However, the effect on individual signatures is diverse, with some signatures captured to a better degree, while others could be reproduced less well.

Figure 10a shows that the Treene, Orge and Loisach benefit the most from the addition of sub-grid heterogeneity. Especially the Treene has a rather large probability of improvement for most of the signatures. This supports the previous findings that the wetland related processes, which are added in mHMtopo, are important to consider in this wet, peaty catchment.

It is interesting to note that the Orge and Loisach, which showed a considerable decrease in performance in terms of the four calibration objective functions (Fig. 6), now exhibit relatively high probabilities of improvement with respect to the signatures when sub-grid heterogeneity is added (Fig. 10a). The signatures with the strongest improvements are related to peaks in the low flow period. Similar to the Treene, the low flow processes are better captured with mHMtopo. The relatively large urban area in the Orge may merely affect the fast, high flow processes, which leads to low performances for  $E_{NS,Q}$  in mHMtopo. Nevertheless, a large area of the Orge catchment is still classified as wetland (see also Fig. 1), adding several processes that only become dominant in the dry periods. Thus, the low flow peaks may be more adequately represented in mHMtopo. Besides, the information of low flow peaks is fully masked when looking at, for example,  $E_{NS,Q}$  or  $E_{NS,\log Q}$ , as the relative importance of peaks in low flows in these metrics is low. First, these metrics consider the whole period of interest, instead of only the low flow period, and, second, the peaks are relatively small compared to the average high flows. Hence, high performances in terms of  $E_{NS,Q}$  or  $E_{NS,\log Q}$  may be misleading, which is very relevant for automatic calibration schemes that often optimize towards these functions. Improvements in, for example, low flow peaks, may remain unnoticed when calibrating on more general objective functions, such as  $E_{NS,Q}$ , as they mostly rely on the absolute values of model residuals aggregated over the entire model period. This is the result of the frequent absence of homoscedasticity in the model residuals. Therefore, errors in high flows tend to have a higher weight in the objective function than errors in low flows. For the Loisach, the findings are also in agreement with findings of

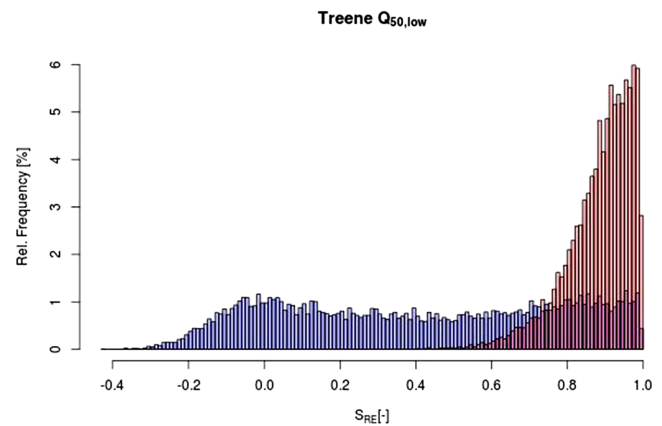


**Figure 11.** Histograms of the performance distributions for the median of the low flows  $Q_{50,low}$  for the Treene catchment on the basis of all feasible parameter sets of mHM (blue) and mHMtopo (red). The performance  $S_{RE}$  is defined as 1 minus the relative error, leading to an optimal value of 1.

Velázquez et al. (2013) that in particular the performance of low flows depends on the choice of the hydrological model. Apparently, here the low flow processes are not easy to capture, as in most hydrological models.

Results for the comparative analysis of the individual signatures instead of catchments indicated a considerable degree of improvement for mHMtopo to represent low flows ( $Q_{50,low}$ ,  $Q_{95,low}$ ,  $Q_{5,low}$ ) and peaks during low flows ( $Q_{peak,10}$ ,  $Q_{low,peak,50}$ ), as can be seen in Fig. 10a. A probability distribution of the performance metric of a signature, so  $S_{RE}$  or  $S_{NS}$ , may indicate whether the feasible space produces many solutions close to optimal. Ideally, a high peak of the distribution function close to 1 indicates a strong ability of the model to reproduce a certain signature, whereas a flat and widespread distribution or even negative performance values indicates a more reduced ability to reproduce the signature. Thus, the improved ability of mHMtopo to reproduce low flow signatures becomes more obvious when looking in detail at the probability distributions of, for example,  $Q_{50,low}$  in the Treene catchment (Fig. 11). The original model of mHM only allows downward percolation and infiltration, which leads to a larger buffer for soil moisture in dry periods. mHMtopo, on the other hand, sustains a shallow groundwater table in wetlands through an upward flux, which leads to a faster response and thus to a better representation of the peaks during dry periods.

In contrast, the 1-day autocorrelations for the total, low flow and high flow periods are consistently better represented in the original mHM (Fig. 10a, b). This indicates that the timing of the flow peaks is better represented in the original model. Likewise, the rising and declining limb densities (RLD and DLD, respectively) are also better captured by the original mHM. Similar to the observation that mHM better captures the fast spiky peaks in the Orge catchment, this sug-

gests again that the simpler model structure (mHM) is able to respond faster, while the more complex model structure (mHMtopo) tends to delay the flow of water. A possible explanation for this observation is that the more complex model has more options, in terms of reservoirs, for storing the water. As linear reservoirs keep draining, the use of multiple reservoirs can produce a delayed and flattened signal. In addition, as the flood peaks now consist of contributions of the different reservoirs, more solutions exist to reconstruct these flood peaks. These solutions could also contain flatter, delayed peaks which affect the 1-day autocorrelation. More specifically, for fast responding catchments like the Orge and Loisach, it means a poor representation of the 1-day autocorrelation in mHMtopo, which offers more storage possibilities and thus more “memory” in the system. However, a closer look at the distributions in detail shows that these differences are small. As an example, Fig. 12 shows the 1-day autocorrelation distributions for the Loisach catchment. Here, it is apparent that the distributions of mHM and mHMtopo are in accordance.

The findings presented here are in line with some other comparison studies, such as Reed et al. (2004), Nicolle et al. (2014), Orth et al. (2015) and te Linde (2008), who all found that added complexity can but does not necessarily lead to improvements. However, in contrast to Orth et al. (2015), we found that low flows are better represented by the complex models, whereas they found that low flows were best represented by a very simple model. Nevertheless, it was stated by Staudinger et al. (2011) that processes in summer low flow periods are more complex due to a stronger interaction between fast storages and evaporation. Therefore, they did not find one particular model structure to represent low flows in summer. In addition, the difficulties in representing low flows have been acknowledged by several authors, such as Smakhtin et al. (2001), Pushpalatha et al. (2011) or Van Esse et al. (2013).

### 3.2.2 Effect of constraints

Figure 10c shows that the addition of prior constraints to mHM strongly improves the signature representation, in particular for, again, the Treene. Apparently, the seasonal runoff constraints help the model to represent the low flows better, which mHMtopo was able to do through the additional processes included. As the upward flux from the groundwater in mHMtopo is counterbalanced in the constrained mHM by different parameters that most likely influence the fast reservoir coefficient and storage, it remains unclear which of the two conceptualizations, i.e. mHM or mHMtopo, is more adequate in this case. Also, the Loisach shows a strong improvement when prior constraints are added to mHM (Fig. 10c). The reasoning considering the importance of snow still holds. The seasonal runoff constraints help to identify parameter sets that are better able to reproduce the seasonal flows, which are strongly affected by snowmelt.

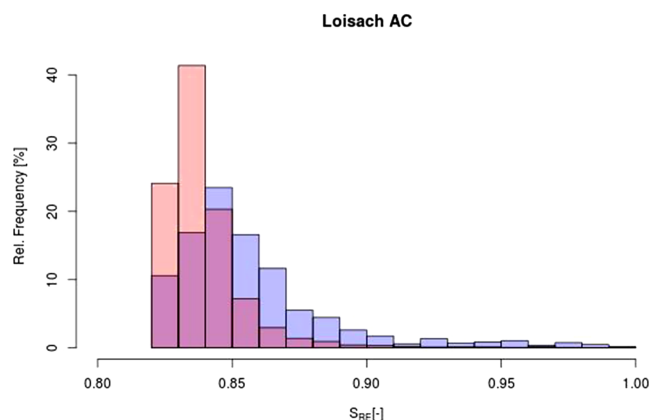


**Figure 12.** Histograms of the performance distributions for the 1-day autocorrelation of flows for the Loisach catchment on the basis of all feasible parameter sets of mHM (blue) and mHMtopo (red). The performance  $E_{RE}$  is defined as 1 minus the relative error, leading to an optimal value of 1.

The additional constraints imposed on mHM do not significantly affect the performance for the Briançonnais and Orge catchment, as can be seen by the nearly white rows in Fig. 10c. Notably, the runoff responses in these catchments are not snow dominated, and as evaporation and rainfall are now out of phase, the original model was already able to capture the seasonality reasonably well.

It can be clearly observed from Fig. 10c, d that the applied prior constraints yield a strong improvement, in particular in mHM, and in only about 29 % (mHM) and 38 % (mHMtopo) of the cases is a mostly weak performance reduction observed. This indicates that, in spite of being constrained by the transfer functions that link parameters to catchment characteristics, additional prior constraints do still contain significant discriminatory information to identify unfeasible model solutions, which is in agreement with findings of Hrachowitz et al. (2014). The picture is less clear for applying constraints to mHMtopo, but improvements are still observed for the majority of the signatures (Fig. 10d; see also the empirical distribution function at the bottom of the figures).

Alzette, Loisach and Orge show some deterioration when constraints are added (Fig. 10d), indicating that the topography specific constraints (Eqs. 4 and 5) may not be fully applicable to these catchments. These catchments show a general decrease in the ability to reproduce several signatures when comparing the unconstrained mHMtopo with the constrained case (Fig. 10d). This means that the unconstrained mHMtopo and also the constrained mHM, which does not have these topography specific constraints, will outperform the constrained mHMtopo with respect to these signatures. This is also supported by Fig. 10b, which illustrates that for the Alzette, Loisach and Orge, the addition of constraints to mHMtopo leads to a reduced ability to represent most signatures compared to the constrained mHM case (see the red

pattern in Fig. 10b). The rejection of these constraints implies that for these catchments, soil moisture storage capacity in wetlands may be equal to or even larger than soil moisture storage capacity in the hillslope and plateau area. This may be true for the Loisach, especially as Kunstmann et al. (2006) found that the karstic nature in these areas even leads to water flowing from the neighbouring Ammer catchment to the Loisach. Considering these groundwater leakages, the model may need extra storage to correct for it in the hydrograph.

In Fig. 10c, d it may also be noted that the constraints do not add information to mHM and mHMtopo with respect to the autocorrelation functions ( $AC$ ,  $AC_{low}$ ,  $AC_{high}$ ) and rising and declining limb densities ( $RLD$ ,  $DLD$ ). This makes sense as the applied constraints here merely affect the seasonal patterns. Therefore, improvements can be observed for signatures addressing low and high flow periods, such as  $Q_{low,95}$  and  $Q_{high,95}$ .

Figure 10d shows that none of the signatures consistently improves or deteriorates. This indicates that care must be taken by including more specific expert knowledge constraints. General constraints, like the runoff constraints, can easily be applied to multiple catchments and lead to improvements as Fig. 10c shows, but assumptions about internal model behaviour should experimentally be well founded. Even though based on several experimental studies, the topography-based parameter constraints applied (Eqs. 4 and 5) were not suitable in all cases, and led to a random pattern of individual signature improvements/deterioration. Thus, it was expected that additional constraints should narrow down the “plausible” parameter space and would lead to more pronounced differences in performances. Nevertheless, the results merely support findings of Holländer et al. (2009), where different choices of expert modellers lead to a variety of outcomes.

### 3.2.3 Combined effect of constraints and sub-grid heterogeneity

Figure 10b shows the effect of additional sub-grid variability on the constrained models. Most of the catchments show a slight overall improvement, indicated by the relatively blue shades for Euclidian distance. In general, the patterns observed in Fig. 10b are relatively similar to the patterns observed in Fig. 10a. It seems that the applied constraints generally enhance the effects caused by the model structure. This can be seen from darker colours of red and blue, but also from the flatter distribution function (bottom of Fig. 10b). Thus, when the model already has a relatively large probability of improvement for certain signatures, the constraints help to zoom in on the good solutions. When this is not the case, the model drifts further away.

Nevertheless, the Briance and Broye show a more different effect, indicating a positive effect of the constraints for mHMtopo. For the Briance, a red box for the Euclidian distance in Fig. 10a turned blue in Fig. 10b. The Broye

gained higher probabilities of improvement, represented by more darker blue colours in Fig. 10b. Apparently, the solutions maintained for the unconstrained mHMtopo case still contained a relatively large number of implausible solutions. Here, the application of constraints helped to narrow the solution space in such a way that mHMtopo showed improvements compared with the original mHM.

However, it must be noted that the Alzette, Loisach and Orge show a relatively low probability of improvement again. This is due to the rejection of the constraints given in Eqs. (4) and (5), as discussed before in comparison with Fig. 10d.

Figure 10e shows the combined effect of constraints and sub-grid heterogeneity on the signature representation compared with the original, unconstrained mHM. The Euclidian distance in the last column of Fig. 10e shows again that most catchments profit from the addition of constraints and sub-grid heterogeneity to mHM. It was noted before that mHMtopo has an improved ability to represent the low flow statistics, whereas the original mHM better represented fast flows signatures like rising limb density ( $RLD$ ) or autocorrelation ( $AC$ ). In Fig. 10e, even a further contrast between the fast flow and low flow domains can be observed. More particular, the Treene again shows the most improvements. The rejection of the topography specific constraints in the Alzette, Loisach and Orge introduce also in Fig. 10e a redder pattern. Nevertheless, the overall improvements in the low flow domains still lead to a general improvement in the Euclidian distance  $D_E$  for the Alzette and Loisach. Only for the Orge catchment, influenced largely by human disturbances, does the Euclidian distance  $D_E$  show a clear deterioration in performance.

## 3.3 Transferability comparison

In a next step, the two models mHM and mHMtopo were calibrated simultaneously on the four catchments Orge, Treene, Broye and Loisach. The parameters were then transferred without further calibration to the three remaining receiver catchments Alzette, Briance and Kinzig. As shown in Fig. 13, both models provide a relatively good performance in the validation period with respect to all four calibration objective functions in the receiver catchments as compared to the individual calibration for the same catchments. Compared with the base case of mHM, the Euclidian distances obtained from the calibration objective functions values changed by 2 % (mHM with constraints), −4 % (mHMtopo) and 1 % (mHMtopo with constraints). The Euclidian distances for the signatures improved by 2 % for the constrained mHM case. However, mHMtopo had a decrease of 5 % and the Euclidian distance almost doubled for the constrained mHMtopo case.

### 3.3.1 Effect of sub-grid heterogeneity

In general, mHM and mHMtopo showed a considerable ability to reproduce similar objective function values as in the

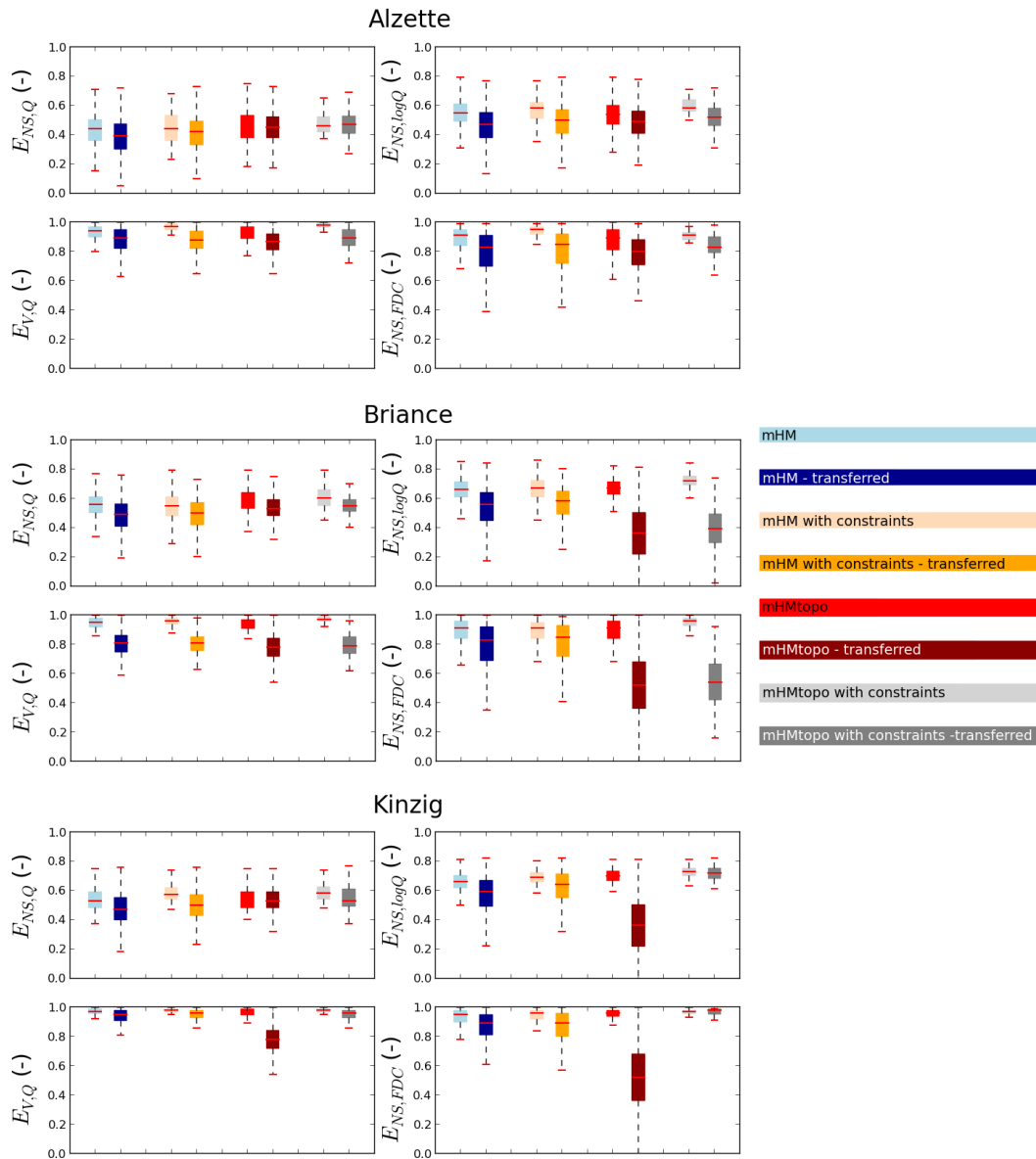


**Figure 13.** Objective function values of the (a) Alzette, (b) Briance and (c) Kinzig catchments in the validation period for individual calibration (light colours) and when using parameters transferred from the remaining four donor catchments in the multibasin calibration (darker colours).

individual calibrations (Fig. 13). Both models kept a reasonable performance during validation in terms of the objective function values and did not fail in reproducing the hydrograph with the parameters received from the donor catchments.

For the Alzette, the results obtained with mHM (blue in Fig. 13) and mHMtopo (red in Fig. 13) are almost identical. For the Briance and Kinzig catchments it is noted that the introduction of sub-grid process heterogeneity, i.e. mHMtopo, leads to a less transferable model. In particular,  $E_{NS,logQ}$  and  $E_{NS,FDC}$  experience a strong decrease in performance (Fig. 13). The results also suggest that, in the unconstrained

case, the original mHM is better transferable than mHMtopo with respect to catchment signatures (Fig. 14a). Most signatures show a low probability of improvement; only some signatures that consider peaks during the low flow periods have a relatively high (blue pattern in Fig. 14a) probability of improvement. This indicates again that the more complex mHMtopo mostly affects the low flows.

It should be noted that the transfer functions used in mHMtopo were adopted for similar parameters from the original mHM. However, it may well be that the assumed functional relations are less valid in a more complex setting. The MPR was developed around the simple model structure and also

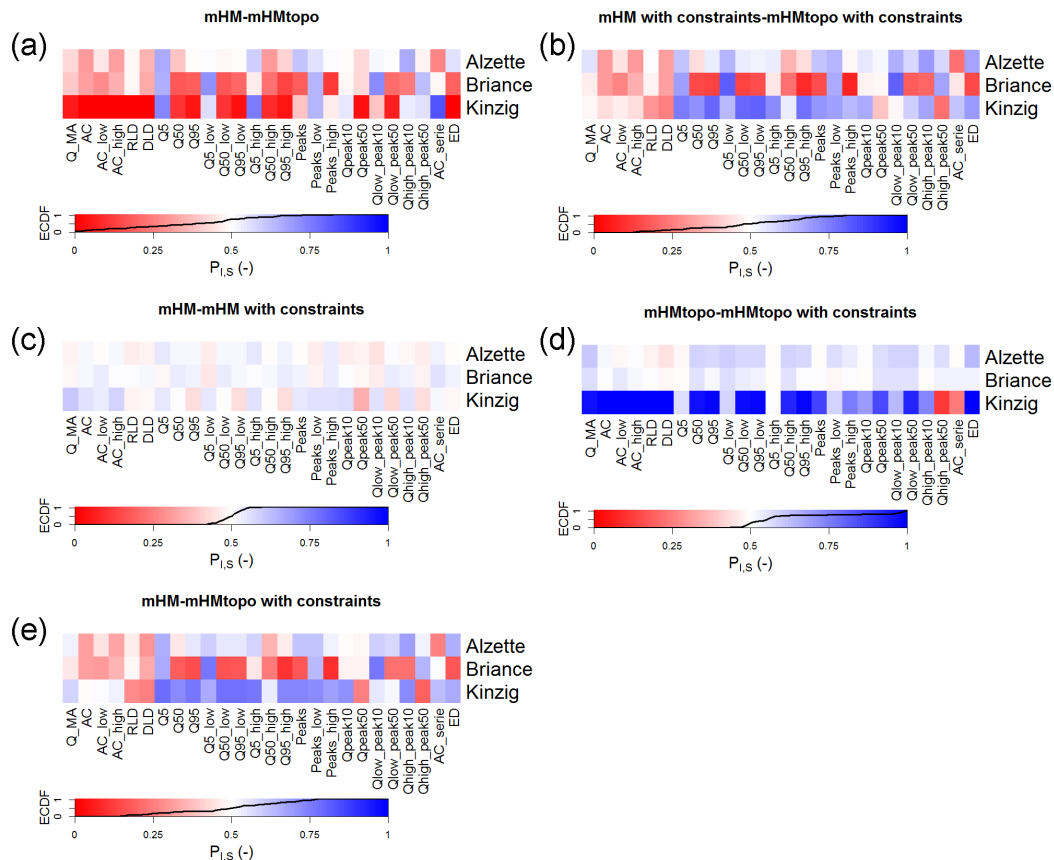


**Figure 14.** Probabilities of improvements  $P_{I,S}$  between (a) mHM and mHMtopo without constraints and (b) with constraints, (c) mHM with and without constraints, (d) mHMtopo with and without constraints and (e) the base case mHM with the constrained mHMtopo case, all after the transfer of global parameters to the three catchments. The colours are linearly related to the probability of improvement between 0 (dark red; e.g. the probability of mHMtopo outperforming mHM is 0), 0.5 (white; i.e. models are statistically equivalent) and 1 (dark blue; e.g. the probability of mHMtopo outperforming mHM is 1). An empirical cumulative distribution function (ECDF) based on all probabilities of improvement has been added to assess the distribution of these probabilities.

refined several times (Samaniego et al., 2010a; Kumar et al., 2013a). Similar efforts are required for refining the regionalization for a topography-driven model in order to make mHMtopo as transferable as the original mHM. In addition, the global parameter ranges that do not have a real physical meaning were also derived for the original mHM and may need adjustments for mHMtopo.

### 3.3.2 Effect of constraints

Imposing prior constraints in mHMtopo leads to a strong increase in performance again in the Kinzig catchment compared to the unconstrained case (Fig. 13). This indicates that the applied constraints are very suitable for this catchment, but less so for the Briance catchment, where only a minor improvement is observed. The Kinzig catchment is characterized by a rather large elevation difference and relatively high contribution of snow, similar to the Loisach catchment. Hence, the same reasoning for this catchment holds as for

the Loisach catchment that the seasonal runoff constraints help in the seasonal flow patterns. Besides, the role of the input data may likely influence the modelling results for this catchment, since the Kinzig catchment has a large difference in elevation.

When comparing the signatures for the constrained mHM and mHMtopo (Fig. 14b), it can be observed that the Alzette and Kinzig catchments benefit from additional process heterogeneity and constraints, while the constrained mHM is still better at representing the signatures in the Briance catchment. In general, the constraints do not have much influence on the Briance catchment, as indicated by a relatively white row in Fig. 14c and d. The unconstrained mHM already was better transferable for this catchment compared to mHMtopo (see Fig. 14a); this remains the same in the constrained cases. The other two catchments are much more sensitive to the constraints and now show a better transferability, in particular with respect to the low flow signatures.



Furthermore, results shown in Fig. 14c and d suggest that prior constraints can add transferability to both models in terms of signatures as highlighted by the probability of improvements for most signatures. For the Kinzig catchment the constrained mHMtopo model is clearly better transferable than the unconstrained mHMtopo as well as mHM with constraints. This was already noted before, when looking at the performances (Fig. 13), but it is here confirmed for the signatures.

In general, it can be stated that the addition of topography-guided sub-grid process heterogeneity per se does not necessarily lead to a pronounced difference in model transferability in all parts of flow regimes. Some improvements were noticed in low flow signature measures. Significant improvements can rather be observed when applying constraints, as illustrated in Fig. 14c, d. The addition of constraints to mHMtopo shows high probabilities of improvements over the full range of signatures (Fig. 14d), in particular for the Kinzig. Also, for mHM (Fig. 14c), even though more moderate, most of the signatures show a relatively large probability of improvement when applying constraints. This test of model transferability underlines the considerable potential of prior constraints to improve the representation of hydrological signatures.

### 3.3.3 Effect of constraints and sub-grid heterogeneity

In the transferability test, Alzette and Kinzig have an improved signature representation in terms of the Euclidian distance when constraints and sub-grid heterogeneity both are added to mHM, as can be seen in Fig. 14e. For these catchments, the biggest improvements, compared with the base case of the unconstrained mHM, are again observed for the low flow statistics.

The Briance catchment shows a general decrease in the ability to represent the signatures. The constraints did not help here (white rows in Fig. 14d) and from Fig. 14a it was already observed that the unconstrained mHM was more transferable than mHMtopo. Looking back at Fig. 10a, it can also be noted that in the individual calibration mHM slightly outperformed mHMtopo for this catchment with respect to the signatures (light-red Euclidian distance). This indicates that the processes in mHMtopo may not adequately represent the processes in this catchment, which is emphasized when the model receives the parameters derived in other catchments. In addition, the derived global relations may not hold for this catchment. Apparently, this catchment, which is gently sloped with agriculture, is significantly different from the other catchments used in calibration. The calibration catchments of Loisach and Broye are more mountainous catchments, whereas the Treene is very flat and wetland dominated. In nature, the Orge catchment should be relatively similar, but this catchment is strongly affected by urbanization.

### 3.4 General limitations and outlook

It should be noted that the input data may have a big influence on the experiment. For example, the input resolution of the E-OBS forcing data is 24 km by 24 km, while the catchments are relatively small. In a few cases, the catchments are just covered by a couple of E-OBS data cells. In addition, as the E-OBS data are a product derived from the interpolation of station data, peaks in rainfall may have been averaged out. In such cases, the detailed process representation in mHMtopo may thus not be warranted. Due to pronounced topography-induced precipitation heterogeneity (e.g. Hrachowitz and Weiler, 2011), this will be more problematic for catchments with marked relief than for catchments that are characterized by a more subdued topography. For example, the Treene benefits most from mHMtopo and is very flat, whereas the steep Loisach needs additional constraints.

In addition to this, one may wonder what the effect of a different spatial model resolution would be. In the extreme case where one modeling cell could be classified as a certain landscape as a whole, the relative importance of the different processes in mHMtopo will increase. Thus, when the assumed processes in the cell are adequate, the performance will increase. Nevertheless, incorrect functional relations may also become more apparent on finer modelling scales, as less up-scaling is required.

The assumptions made in the applied functional relationships may also affect the outcomes of this experiment. In future work, these relationship may need refinement for mHMtopo. Besides this, the threshold values to delineate the landscape units were originally derived for one specific catchment. The general validity of these thresholds needs to be tested in future research.

## 4 Conclusions

In this study the value of incorporating topography-controlled sub-grid process heterogeneity together with semi-quantitative model constraints to increase hydrological consistency and spatial transferability of the the distributed, conceptual model mHM was tested. Both the unconstrained and constrained applications of the original mHM and the topography-based mHMtopo were applied to seven distinct catchments across Europe.

On balance, the addition of topography-based sub-grid process heterogeneity moderately improved mHM. Different hydrological signatures indicated that in particular the representation of low flows improved by allowing for increased sub-grid process heterogeneity. This could be attributed mostly to additional processes which were missing in the original mHM. Especially in catchments where the process of capillary rise is likely to be more important, it became clear that low flows' signatures were better repre-

sented. Nevertheless, the timing of flow peaks was better captured by the original mHM model. In summary, the addition of topography-based sub-grid process heterogeneity in the model structure of a distributed model regionalized through soil and land use was to a moderate degree able to improve the general model performance in the study catchments while more adequately reflecting internal processes.

The use of prior, semi-quantitative constraints proved highly effective in the study catchments as it forces the model to reproduce plausible patterns of partitioning between runoff and evaporative fluxes. Especially in cases where runoff and evaporation are out of phase, the constraints were shown to be valuable. These conclusions were largely drawn from the models' varying ability to reproduce observed catchment signatures.

In addition, it was shown that such an improved hydrological consistency at the sub-grid scale, combined with the use of suitable model constraints and functional relationships, can be beneficial for transferring models and predicting flows without further calibration in other catchments.

In conclusion, the addition of topography-based sub-grid process heterogeneity and the use of prior semi-quantitative constraints were shown to be promising and lead to moderate improvements in terms of process representation and transferability.

**The Supplement related to this article is available online at doi:10.5194/hess-20-1151-2016-supplement.**

**Acknowledgements.** We would like to acknowledge European Commission FP7 funded research project Sharing Water-related Information to Tackle Changes in the Hydrosphere-for Operational Needs (SWITCH-ON, grant agreement number 603587), as this study was conducted within the context of SWITCH-ON.

We acknowledge the E-OBS data set from the ENSEMBLES EU-FP6 project (<http://ensembles-eu.metoffice.com>) and the data providers in the ECA&D project (<http://www.ecad.eu>).

We acknowledge the Global Runoff Data Centre, 56002 Koblenz, Germany, for providing discharge data.

Edited by: E. Zehe

## References

- Abdulla, F. A. and Lettenmaier, D. P.: Development of regional parameter estimation equations for a macroscale hydrologic model, *J. Hydrol.*, 197, 230–257, doi:10.1016/S0022-1694(96)03262-3, 1997.
- Andréassian, V., Perrin, C., Berthet, L., Le Moine, N., Lerat, J., Loumagne, C., Oudin, L., Mathevet, T., Ramos, M.-H., and Valéry, A.: HESS Opinions “Crash tests for a standardized evaluation of hydrological models”, *Hydrol. Earth Syst. Sci.*, 13, 1757–1764, doi:10.5194/hess-13-1757-2009, 2009.
- Andréassian, V., Le Moine, N., Perrin, C., Ramos, M.-H., Oudin, L., Mathevet, T., Lerat, J., and Berthet, L.: All that glitters is not gold: the case of calibrating hydrological models, *Hydrol. Process.*, 26, 2206–2210, doi:10.1002/hyp.9264, 2012.
- Arino, O., Ramos, J., Kalogirou, V., Defourny, P., and Achard, F.: GlobCover, ESA Living Planet Symposium, 27 June–2 July 2010, Bergen, Norway, 2009.
- Bergström, S.: The HBV model: Its structure and applications, Swedish Meteorological and Hydrological Institute, Norrköping, 1–33, 1992.
- Beven, K. J.: Prophecy, reality and uncertainty in distributed hydrological modelling, *Adv. Water Resour.*, 16, 41–51, doi:10.1016/0309-1708(93)90028-E, 1993.
- Beven, K. J.: Uniqueness of place and process representations in hydrological modelling, *Hydrol. Earth Syst. Sci.*, 4, 203–213, doi:10.5194/hess-4-203-2000, 2000.
- Beven, K. J.: A manifesto for the equifinality thesis, *J. Hydrol.*, 320, 18–36, doi:10.1016/j.jhydrol.2005.07.007, 2006.
- Beven, K. J. and Kirkby, M. J.: A physically based, variable contributing area model of basin hydrology/Un modèle à base physique de zone d'appel variable de l'hydrologie du bassin versant, *Hydrol. Sci. Bull.*, 24, 43–69, doi:10.1080/02626667909491834, 1979.
- Booij, M.: Impact of climate change on river flooding assessed with different spatial model resolutions, *J. Hydrol.*, 303, 176–198, doi:10.1016/j.jhydrol.2004.07.013, 2005.
- Coron, L., Andréassian, V., Perrin, C., Lerat, J., Vaze, J., Bourqui, M., and Hendrickx, F.: Crash testing hydrological models in contrasted climate conditions: An experiment on 216 Australian catchments, *Water Resour. Res.*, 48, W05552, doi:10.1029/2011WR011721, 2012.
- Das, T., Bárdossy, A., Zehe, E., and He, Y.: Comparison of conceptual model performance using different representations of spatial variability, *J. Hydrol.*, 356, 106–118, doi:10.1016/j.jhydrol.2008.04.008, 2008.
- Detty, J. M. and McGuire, K. J.: Topographic controls on shallow groundwater dynamics: implications of hydrologic connectivity between hillslopes and riparian zones in a till mantled catchment, *Hydrol. Process.*, 24, 2222–2236, doi:10.1002/hyp.7656, 2010.
- Duan, Q., Sorooshian, S., and Gupta, V.: Effective and efficient global optimization for conceptual rainfall-runoff models, *Water Resour. Res.*, 28, 1015–1031, doi:10.1029/91WR02985, 1992.
- Eder, G., Sivapalan, M., and Nachtnebel, H. P.: Modelling water balances in an Alpine catchment through exploitation of emergent properties over changing time scales, *Hydrol. Process.*, 17, 2125–2149, doi:10.1002/hyp.1325, 2003.
- Euser, T., Winsemius, H. C., Hrachowitz, M., Fenicia, F., Uhlenbrook, S., and Savenije, H. H. G.: A framework to assess the realism of model structures using hydrological signatures, *Hydrol. Earth Syst. Sci.*, 17, 1893–1912, doi:10.5194/hess-17-1893-2013, 2013.
- Euser, T., Hrachowitz, M., Winsemius, H. C., and Savenije, H. H. G.: The effect of forcing and landscape distribution on performance and consistency of model structures, *Hydrol. Process.*, 29, 3727–3743, doi:10.1002/hyp.10445, 2015.
- FAO/IIASA/ISRIC/ISSCAS/JRC: Harmonized World Soil Database (version 1.2), Rome, Laxenburg, 2012.
- Fenicia, F., Savenije, H. H. G., Matgen, P., and Pfister, L.: Understanding catchment behavior through stepwise model

- concept improvement, *Water Resour. Res.*, 44, W01402, doi:10.1029/2006WR005563, 2008.
- Flügel, W.-A.: Delineating hydrological response units by geographical information system analyses for regional hydrological modelling using PRMS/MMS in the drainage basin of the River Bröl, Germany, *Hydrol. Process.*, 9, 423–436, doi:10.1002/hyp.3360090313, 1995.
- Fovet, O., Ruiz, L., Hrachowitz, M., Faucheux, M., and Gascuel-Odoux, C.: Hydrological hysteresis and its value for assessing process consistency in catchment conceptual models, *Hydrol. Earth Syst. Sci.*, 19, 105–123, doi:10.5194/hess-19-105-2015, 2015.
- Gao, H., Hrachowitz, M., Fenicia, F., Gharari, S., and Savenije, H. H. G.: Testing the realism of a topography-driven model (FLEX-Topo) in the nested catchments of the Upper Heihe, China, *Hydrol. Earth Syst. Sci.*, 18, 1895–1915, doi:10.5194/hess-18-1895-2014, 2014a.
- Gao, H., Hrachowitz, M., Schymanski, S. J., Fenicia, F., Sriwongsitanton, N., and Savenije, H. H. G.: Climate controls how ecosystems size the root zone storage capacity at catchment scale, *Geophys. Res. Lett.*, 41, 7916–7923, doi:10.1002/2014GL061668, 2014b.
- Gharari, S., Hrachowitz, M., Fenicia, F., and Savenije, H. H. G.: Hydrological landscape classification: investigating the performance of HAND based landscape classifications in a central European meso-scale catchment, *Hydrol. Earth Syst. Sci.*, 15, 3275–3291, doi:10.5194/hess-15-3275-2011, 2011.
- Gharari, S., Hrachowitz, M., Fenicia, F., Gao, H., and Savenije, H. H. G.: Using expert knowledge to increase realism in environmental system models can dramatically reduce the need for calibration, *Hydrol. Earth Syst. Sci.*, 18, 4839–4859, doi:10.5194/hess-18-4839-2014, 2014.
- Göttinger, J. and Bárdossy, A.: Comparison of four regionalisation methods for a distributed hydrological model, *J. Hydrol.*, 333, 374–384, doi:10.1016/j.jhydrol.2006.09.008, 2007.
- Gupta, H. V., Wagener, T., and Liu, Y.: Reconciling theory with observations: elements of a diagnostic approach to model evaluation, *Hydrol. Process.*, 22, 3802–3813, doi:10.1002/hyp.6989, 2008.
- Gupta, H. V., Clark, M. P., Vrugt, J. A., Abramowitz, G., and Ye, M.: Towards a comprehensive assessment of model structural adequacy, *Water Resour. Res.*, 48, W08301, doi:10.1029/2011WR011044, 2012.
- Hargreaves, G. H. and Samani, Z. A.: Reference crop evapotranspiration from ambient air temperature, American Society of Agricultural Engineers, Microfiche collection, USA, no. 85-2517, Chicago, 1985.
- Haylock, M., Hofstra, N., Klein Tank, A., Klok, E., Jones, P., and New, M.: A European daily high-resolution gridded data set of surface temperature and precipitation for 1950–2006, *J. Geophys. Res.-Atmos.*, 113, D20119, doi:10.1029/2008JD010201, 2008.
- Holländer, H. M., Blume, T., Bormann, H., Buytaert, W., Chirico, G., Exbrayat, J.-F., Gustafsson, D., Hölzel, H., Kraft, P., Stamm, C., Stoll, S., Blöschl, G., and Flüher, H.: Comparative predictions of discharge from an artificial catchment (Chicken Creek) using sparse data, *Hydrol. Earth Syst. Sci.*, 13, 2069–2094, doi:10.5194/hess-13-2069-2009, 2009.
- Hrachowitz, M. and Weiler, M.: Uncertainty of Precipitation Estimates Caused by Sparse Gauging Networks in a Small, Mountainous Watershed, *J. Hydrol. Eng.*, 16, 460–471, doi:10.1061/(ASCE)HE.1943-5584.0000331, 2011.
- Hrachowitz, M., Fovet, O., Ruiz, L., Euser, T., Gharari, S., Nijzink, R., Freer, J., Savenije, H. H. G., and Gascuel-Odoux, C.: Process consistency in models: The importance of system signatures, expert knowledge, and process complexity, *Water Resour. Res.*, 50, 7445–7469, doi:10.1002/2014WR015484, 2014.
- Hughes, D.: A review of 40 years of hydrological science and practice in southern Africa using the Pitman rainfall runoff model, *J. Hydrol.*, 501, 111–124, doi:10.1016/j.jhydrol.2013.07.043, 2013.
- Hundecha, Y. and Bárdossy, A.: Modeling of the effect of land use changes on the runoff generation of a river basin through parameter regionalization of a watershed model, *J. Hydrol.*, 292, 281–295, doi:10.1016/j.jhydrol.2004.01.002, 2004.
- Jencso, K. G., McGlynn, B. L., Gooseff, M. N., Wondzell, S. M., Bencala, K. E., and Marshall, L. A.: Hydrologic connectivity between landscapes and streams: Transferring reach- and plot-scale understanding to the catchment scale, *Water Resour. Res.*, 45, W04428, doi:10.1029/2008WR007225, 2009.
- Jothityangkoon, C., Sivapalan, M., and Farmer, D.: Process controls of water balance variability in a large semi-arid catchment: downward approach to hydrological model development, *J. Hydrol.*, 254, 174–198, doi:10.1016/S0022-1694(01)00496-6, 2001.
- Kapangaziwiri, E., Hughes, D., and Wagener, T.: Incorporating uncertainty in hydrological predictions for gauged and ungauged basins in southern Africa, *Hydrol. Sci. J.*, 57, 1000–1019, doi:10.1080/02626667.2012.690881, 2012.
- Kirchner, J. W.: Getting the right answers for the right reasons: Linking measurements, analyses, and models to advance the science of hydrology, *Water Resour. Res.*, 42, W03S04, doi:10.1029/2005WR004362, 2006.
- Kite, G. W. and Kouwen, N.: Watershed modeling using land classifications, *Water Resour. Res.*, 28, 3193–3200, doi:10.1029/92WR01819, 1992.
- Knudsen, J., Thomsen, A., and Refsgaard, J. C.: WATBAL, *Nord. Hydrol.*, 17, 347–362, 1986.
- Kouwen, N., Soulis, E., Pietroniro, A., Donald, J., and Harrington, R.: Grouped Response Units for Distributed Hydrologic Modeling, *J. Water Resour. Plan. Manage.*, 119, 289–305, doi:10.1061/(ASCE)0733-9496(1993)119:3(289), 1993.
- Kumar, P.: Typology of hydrologic predictability, *Water Resour. Res.*, 47, W00H05, doi:10.1029/2010WR009769, 2011.
- Kumar, R., Samaniego, L., and Attinger, S.: The effects of spatial discretization and model parameterization on the prediction of extreme runoff characteristics, *J. Hydrol.*, 392, 54–69, doi:10.1016/j.jhydrol.2010.07.047, 2010.
- Kumar, R., Livneh, B., and Samaniego, L.: Toward computationally efficient large-scale hydrologic predictions with a multi-scale regionalization scheme, *Water Resour. Res.*, 49, 5700–5714, doi:10.1002/wrcr.20431, 2013a.
- Kumar, R., Samaniego, L., and Attinger, S.: Implications of distributed hydrologic model parameterization on water fluxes at multiple scales and locations, *Water Resour. Res.*, 49, 360–379, doi:10.1029/2012WR012195, 2013b.

- Kunstmann, H., Krause, J., and Mayr, S.: Inverse distributed hydrological modelling of Alpine catchments, *Hydrol. Earth Syst. Sci.*, 10, 395–412, doi:10.5194/hess-10-395-2006, 2006.
- Leavesley, G. and Stannard, L.: Application of remotely sensed data in a distributed-parameter watershed model, *Application of Remote Sensing in Hydrology*, Saskatoon, 47–68, 1990.
- Lehner, B., Verdin, K., and Jarvis, A.: New global hydrography derived from spaceborne elevation data, *EOS, Trans. Am. Geophys. Union*, 89, 93–94, 2008.
- Liang, X., Lettenmaier, D. P., Wood, E. F., and Burges, S. J.: A simple hydrologically based model of land surface water and energy fluxes for general circulation models, *J. Geophys. Res.-Atmos.*, 99, 14415–14428, doi:10.1029/94JD00483, 1994.
- Lindström, G., Pers, C., Rosberg, J., Stromqvist, J., and Arheimer, B.: Development and testing of the HYPE (Hydrological Predictions for the Environment) water quality model for different spatial scales, *Hydrol. Res.*, 41, 295–319, doi:10.2166/nh.2010.007, 2010.
- Livneh, B., Kumar, R., and Samaniego, L.: Influence of soil textural properties on hydrologic fluxes in the Mississippi river basin, *Hydrol. Process.*, 29, 4638–4655, doi:10.1002/hyp.10601, 2015.
- McGlynn, B. L., McDonnell, J. J., Seibert, J., and Kendall, C.: Scale effects on headwater catchment runoff timing, flow sources, and groundwater-streamflow relations, *Water Resour. Res.*, 40, W07504, doi:10.1029/2003WR002494, 2004.
- Merz, B. and Bárdossy, A.: Effects of spatial variability on the rainfall runoff process in a small loess catchment, *J. Hydrol.*, 212–213, 304–317, doi:10.1016/S0022-1694(98)00213-3, 1998.
- Montanari, A. and Toth, E.: Calibration of hydrological models in the spectral domain: An opportunity for scarcely gauged basins?, *Water Resour. Res.*, 43, W05434, doi:10.1029/2006WR005184, 2007.
- Mou, L., Tian, F., Hu, H., and Sivapalan, M.: Extension of the Representative Elementary Watershed approach for cold regions: constitutive relationships and an application, *Hydrol. Earth Syst. Sci.*, 12, 565–585, doi:10.5194/hess-12-565-2008, 2008.
- Muerth, M. J., Gauvin St-Denis, B., Ricard, S., Velázquez, J. A., Schmid, J., Minville, M., Caya, D., Chaumont, D., Ludwig, R., and Turcotte, R.: On the need for bias correction in regional climate scenarios to assess climate change impacts on river runoff, *Hydrol. Earth Syst. Sci.*, 17, 1189–1204, doi:10.5194/hess-17-1189-2013, 2013.
- Nicollé, P., Pushpalatha, R., Perrin, C., François, D., Thiéry, D., Mathevet, T., Le Lay, M., Besson, F., Soubeyroux, J.-M., Viel, C., Regimbeau, F., Andréassian, V., Maugis, P., Augeard, B., and Morice, E.: Benchmarking hydrological models for low-flow simulation and forecasting on French catchments, *Hydrol. Earth Syst. Sci.*, 18, 2829–2857, doi:10.5194/hess-18-2829-2014, 2014.
- Nobre, A., Cuartas, L., Hodnett, M., Rennó, C., Rodrigues, G., Silveira, A., Waterloo, M., and Saleska, S.: Height Above the Nearest Drainage – a hydrologically relevant new terrain model, *J. Hydrol.*, 404, 13–29, doi:10.1016/j.jhydrol.2011.03.051, 2011.
- Obled, C., Wendling, J., and Beven, K.: The sensitivity of hydrological models to spatial rainfall patterns: an evaluation using observed data, *J. Hydrol.*, 159, 305–333, doi:10.1016/0022-1694(94)90263-1, 1994.
- Orth, R., Staudinger, M., Seneviratne, S. I., Seibert, J., and Zappa, M.: Does model performance improve with complexity? A case study with three hydrological models, *J. Hydrol.*, 523, 147–159, doi:10.1016/j.jhydrol.2015.01.044, 2015.
- Pape, P. L., Ayrault, S., and Quantin, C.: Trace element behaviour and partition versus urbanization gradient in an urban river (Orge River, France), *J. Hydrol.*, 472–473, 99–110, doi:10.1016/j.jhydrol.2012.09.042, 2012.
- Perrin, C., Michel, C., and Andréassian, V.: Does a large number of parameters enhance model performance? Comparative assessment of common catchment model structures on 429 catchments, *J. Hydrol.*, 242, 275–301, doi:10.1016/S0022-1694(00)00393-0, 2001.
- Perrin, C., Michel, C., and Andréassian, V.: Improvement of a parsimonious model for streamflow simulation, *J. Hydrol.*, 279, 275–289, doi:10.1016/S0022-1694(03)00225-7, 2003.
- Pokhrel, P., Gupta, H. V., and Wagener, T.: A spatial regularization approach to parameter estimation for a distributed watershed model, *Water Resour. Res.*, 44, W12419, doi:10.1029/2007WR006615, 2008.
- Pushpalatha, R., Perrin, C., Moine, N. L., Mathevet, T., and Andréassian, V.: A downward structural sensitivity analysis of hydrological models to improve lowflow simulation, *J. Hydrol.*, 411, 66–76, doi:10.1016/j.jhydrol.2011.09.034, 2011.
- Rakovec, O., Kumar, R., Mai, J., Cuntz, M., Thober, S., Zink, M., Attinger, S., Schäfer, D., Schrön, M., and Samaniego, L.: Multiscale and multivariate evaluation of water fluxes and states over European river basins, *J. Hydrometeorol.*, 17, 287–307, doi:10.1175/JHM-D-15-0054.1, 2015.
- Reed, S., Koren, V., Smith, M., Zhang, Z., Moreda, F., Seo, D.-J., and Participants, D.: Overall distributed model intercomparison project results, *J. Hydrol.*, 298, 27–60, doi:10.1016/j.jhydrol.2004.03.031, 2004.
- Refsgaard, J. C. and Storm, B.: MIKE SHE, in: *Computer models of watershed hydrology*, edited by: Singh, V. P., Water Resources Publications, Littleton, 809–846, 1995.
- Refsgaard, J. C. and Knudsen, J.: Operational Validation and Intercomparison of Different Types of Hydrological Models, *Water Resour. Res.*, 32, 2189–2202, doi:10.1029/96WR00896, 1996.
- Reggiani, P. and Rientjes, T. H. M.: Flux parameterization in the representative elementary watershed approach: Application to a natural basin, *Water Resour. Res.*, 41, W04013, doi:10.1029/2004WR003693, 2005.
- Reggiani, P., Sivapalan, M., and Hassanizadeh, S. M.: A unifying framework for watershed thermodynamics: balance equations for mass, momentum, energy and entropy, and the second law of thermodynamics, *Adv. Water Resour.*, 22, 367–398, doi:10.1016/S0309-1708(98)00012-8, 1998.
- Reichert, P. and Omlin, M.: On the usefulness of overparameterized ecological models, *Ecol. Model.*, 95, 289–299, doi:10.1016/S0304-3800(96)00043-9, 1997.
- Rennó, C. D., Nobre, A. D., Cuartas, L. A., Soares, J. V., Hodnett, M. G., Tomasella, J., and Waterloo, M. J.: HAND, a new terrain descriptor using SRTM-DEM: Mapping terra-firme rainforest environments in Amazonia, *Remote Sens. Environ.*, 112, 3469–3481, doi:10.1016/j.rse.2008.03.018, 2008.
- Rodríguez-Iturbe, I., Isham, V., Cox, D. R., Manfreda, S., and Porporato, A.: Space-time modeling of soil moisture: Stochastic rainfall forcing with heterogeneous vegetation, *Water Resour. Res.*, 42, W06D05, doi:10.1029/2005WR004497, 2006.

- Samaniego, L., Kumar, R., and Attinger, S.: Multiscale parameter regionalization of a grid-based hydrologic model at the mesoscale, *Water Resour. Res.*, 46, W05523, doi:10.1029/2008WR007327, 2010a.
- Samaniego, L., Bárdossy, A., and Kumar, R.: Streamflow prediction in ungauged catchments using copula-based dissimilarity measures, *Water Resour. Res.*, 46, W02506, doi:10.1029/2008WR007695, 2010b.
- Samaniego, L., Kumar, R., and Zink, M.: Implications of parameter uncertainty on soil moisture drought analysis in Germany, *J. Hydrometeorol.*, 14, 47–68, doi:10.1175/JHM-D-12-075.1, 2013.
- Savenije, H. H. G.: HESS Opinions “Topography driven conceptual modelling (FLEX-Topo)”, *Hydrol. Earth Syst. Sci.*, 14, 2681–2692, doi:10.5194/hess-14-2681-2010, 2010.
- Sawicz, K., Wagener, T., Sivapalan, M., Troch, P. A., and Carrillo, G.: Catchment classification: empirical analysis of hydrologic similarity based on catchment function in the eastern USA, *Hydrol. Earth Syst. Sci.*, 15, 2895–2911, doi:10.5194/hess-15-2895-2011, 2011.
- Schmalz, B. and Fohrer, N.: Comparing model sensitivities of different landscapes using the ecohydrological SWAT model, *Adv. Geosci.*, 21, 91–98, doi:10.5194/adgeo-21-91-2009, 2009.
- Schmalz, B., Tavares, F., and Fohrer, N.: Modelling hydrological processes in mesoscale lowland river basins with SWAT – capabilities and challenges, *Hydrol. Sci. J.*, 53, 989–1000, doi:10.1623/hysj.53.5.989, 2008.
- Schmocker-Fackel, P., Naef, F., and Scherrer, S.: Identifying runoff processes on the plot and catchment scale, *Hydrol. Earth Syst. Sci.*, 11, 891–906, doi:10.5194/hess-11-891-2007, 2007.
- Schoups, G., Hopmans, J. W., Young, C. A., Vrugt, J. A., and Wallender, W. W.: Multi-criteria optimization of a regional spatially-distributed subsurface water flow model, *J. Hydrol.*, 311, 20–48, doi:10.1016/j.jhydrol.2005.01.001, 2005.
- Seibert, J. and McDonnell, J.: Gauging the Ungauged Basin: Relative Value of Soft and Hard Data, *J. Hydrol. Eng.*, A4014004, doi:10.1061/(ASCE)HE.1943-5584.0000861, 2013.
- Seibert, J. and McDonnell, J. J.: On the dialog between experimentalist and modeler in catchment hydrology: Use of soft data for multicriteria model calibration, *Water Resour. Res.*, 38, 23-1–23-14, doi:10.1029/2001WR000978, 2002.
- Seibert, J., Bishop, K., Rodhe, A., and McDonnell, J. J.: Groundwater dynamics along a hillslope: A test of the steady state hypothesis, *Water Resour. Res.*, 39, 1014, doi:10.1029/2002WR001404, 2003a.
- Seibert, J., Rodhe, A., and Bishop, K.: Simulating interactions between saturated and unsaturated storage in a conceptual runoff model, *Hydrol. Process.*, 17, 379–390, doi:10.1002/hyp.1130, 2003b.
- Shamir, E., Imam, B., Morin, E., Gupta, H. V., and Sorooshian, S.: The role of hydrograph indices in parameter estimation of rainfall-runoff models, *Hydrol. Process.*, 19, 2187–2207, doi:10.1002/hyp.5676, 2005.
- Singh, V. P.: Effect of spatial and temporal variability in rainfall and watershed characteristics on stream flow hydrograph, *Hydrol. Process.*, 11, 1649–1669, doi:10.1002/(SICI)1099-1085(19971015)11:12<1649::AID-HYP495>3.0.CO;2-1, 1997.
- Smakhtin, V.: Low flow hydrology: a review, *J. Hydrol.*, 240, 147–186, doi:10.1016/S0022-1694(00)00340-1, 2001.
- Spence, C., Guan, X. J., Phillips, R., Hedstrom, N., Granger, R., and Reid, B.: Storage dynamics and streamflow in a catchment with a variable contributing area, *Hydrol. Process.*, 24, 2209–2221, doi:10.1002/hyp.7492, 2010.
- Staudinger, M., Stahl, K., Seibert, J., Clark, M. P., and Tallaksen, L. M.: Comparison of hydrological model structures based on recession and low flow simulations, *Hydrol. Earth Syst. Sci.*, 15, 3447–3459, doi:10.5194/hess-15-3447-2011, 2011.
- te Linde, A. H., Aerts, J. C. J. H., Hurkmans, R. T. W. L., and Eberle, M.: Comparing model performance of two rainfall runoff models in the Rhine basin using different atmospheric forcing data sets, *Hydrol. Earth Syst. Sci.*, 12, 943–957, doi:10.5194/hess-12-943-2008, 2008.
- Thober, S., Kumar, R., Sheffield, J., Mai, J., Schäfer, D., and Samaniego, L.: Seasonal Soil Moisture Drought Prediction over Europe using the North American Multi-Model Ensemble (NMME), *J. Hydrometeorol.*, 2329–2344, doi:10.1175/JHM-D-15-0053.1, 2015.
- Tian, F., Hu, H., Lei, Z., and Sivapalan, M.: Extension of the Representative Elementary Watershed approach for cold regions via explicit treatment of energy related processes, *Hydrol. Earth Syst. Sci.*, 10, 619–644, doi:10.5194/hess-10-619-2006, 2006.
- Tolson, B. A. and Shoemaker, C. A.: Dynamically dimensioned search algorithm for computationally efficient watershed model calibration, *Water Resour. Res.*, 43, W01413, doi:10.1029/2005WR004723, 2007.
- Tonkin, M. J. and Doherty, J.: A hybrid regularized inversion methodology for highly parameterized environmental models, *Water Resour. Res.*, 41, W10412, doi:10.1029/2005WR003995, 2005.
- Tromp-van Meerveld, H. J. and McDonnell, J. J.: Threshold relations in subsurface stormflow: 2. The fill and spill hypothesis, *Water Resour. Res.*, 42, W02411, doi:10.1029/2004WR003800, 2006.
- Uhlenbrook, S., Roser, S., and Tilch, N.: Hydrological process representation at the meso-scale: the potential of a distributed, conceptual catchment model, *J. Hydrol.*, 291, 278–296, doi:10.1016/j.jhydrol.2003.12.038, 2004.
- van Emmerik, T., Mulder, G., Eilander, D., Piet, M., and Savenije, H.: Predicting the ungauged basin: Model validation and realism assessment, *Front. Earth Sci.*, 3, 62, doi:10.3389/feart.2015.00062, 2015.
- van Esse, W. R., Perrin, C., Booij, M. J., Augustijn, D. C. M., Fenicia, F., Kavetski, D., and Lobligois, F.: The influence of conceptual model structure on model performance: a comparative study for 237 French catchments, *Hydrol. Earth Syst. Sci.*, 17, 4227–4239, doi:10.5194/hess-17-4227-2013, 2013.
- Vannamettee, E., Karssenbergh, D., and Bierkens, M. F. P.: Towards closure relations in the Representative Elementary Watershed (REW) framework containing observable parameters: Relations for Hortonian overland flow, *Adv. Water Resour.*, 43, 52–66, doi:10.1016/j.advwatres.2012.03.029, 2012.
- Velázquez, J. A., Schmid, J., Ricard, S., Muerth, M. J., Gauvin St-Denis, B., Minville, M., Chaumont, D., Caya, D., Ludwig, R., and Turcotte, R.: An ensemble approach to assess hydrological models’ contribution to uncertainties in the analysis of climate change impact on water resources, *Hydrol. Earth Syst. Sci.*, 17, 565–578, doi:10.5194/hess-17-565-2013, 2013.

- Wagener, T. and Gupta, H.: Model identification for hydrological forecasting under uncertainty, *Stochastic Environmental Research and Risk Assessment*, 19, 378–387, doi:10.1007/s00477-005-0006-5, 2005.
- Wigmosta, M. S., Vail, L. W., and Lettenmaier, D. P.: A distributed hydrology-vegetation model for complex terrain, *Water Resour. Res.*, 30, 1665–1679, doi:10.1029/94WR00436, 1994.
- Wilks, D. S.: *Statistical methods in the atmospheric sciences*, vol. 100, Academic Press, Oxford, 351–354, 2011.
- Winsemius, H. C., Savenije, H. H. G., and Bastiaanssen, W. G. M.: Constraining model parameters on remotely sensed evaporation: justification for distribution in ungauged basins?, *Hydrol. Earth Syst. Sci.*, 12, 1403–1413, doi:10.5194/hess-12-1403-2008, 2008.
- Winter, T. C.: THE CONCEPT OF HYDROLOGIC LANDSCAPES1, *J. Am. W. Resour. Assoc.*, 37, 335–349, doi:10.1111/j.1752-1688.2001.tb00973.x, 2001.
- Yilmaz, K. K., Gupta, H. V., and Wagener, T.: A process-based diagnostic approach to model evaluation: Application to the NWS distributed hydrologic model, *Water Resour. Res.*, 44, W09417, doi:10.1029/2007WR006716, 2008.
- Young, P. C.: Parallel Processes in Hydrology and Water Quality: A Unified Time-Series Approach, *Water Environ. J.*, 6, 598–612, doi:10.1111/j.1747-6593.1992.tb00796.x, 1992.
- Zehe, E., Maurer, T., Ihringer, J., and Plate, E.: Modeling water flow and mass transport in a loess catchment, *Phys. Chem. Earth*, 26, 487–507, doi:10.1016/S1464-1909(01)00041-7, 2001.
- Zehe, E., Ehret, U., Pfister, L., Blume, T., Schröder, B., Westhoff, M., Jackisch, C., Schymanski, S. J., Weiler, M., Schulz, K., Allroggen, N., Tronicke, J., van Schaik, L., Dietrich, P., Scherer, U., Eccard, J., Wulfmeyer, V., and Kleidon, A.: HESS Opinions: From response units to functional units: a thermodynamic reinterpretation of the HRU concept to link spatial organization and functioning of intermediate scale catchments, *Hydrol. Earth Syst. Sci.*, 18, 4635–4655, doi:10.5194/hess-18-4635-2014, 2014.
- Zhang, G. P. and Savenije, H. H. G.: Rainfall-runoff modelling in a catchment with a complex groundwater flow system: application of the Representative Elementary Watershed (REW) approach, *Hydrol. Earth Syst. Sci.*, 9, 243–261, doi:10.5194/hess-9-243-2005, 2005.
- Zhang, G. P., Savenije, H. H. G., Fenicia, F., and Pfister, L.: Modelling subsurface storm flow with the Representative Elementary Watershed (REW) approach: application to the Alzette River Basin, *Hydrol. Earth Syst. Sci.*, 10, 937–955, doi:10.5194/hess-10-937-2006, 2006.
- Zhao, R.-J.: The Xinanjiang model applied in China, *J. Hydrol.*, 135, 371–381, doi:10.1016/0022-1694(92)90096-E, 1992.